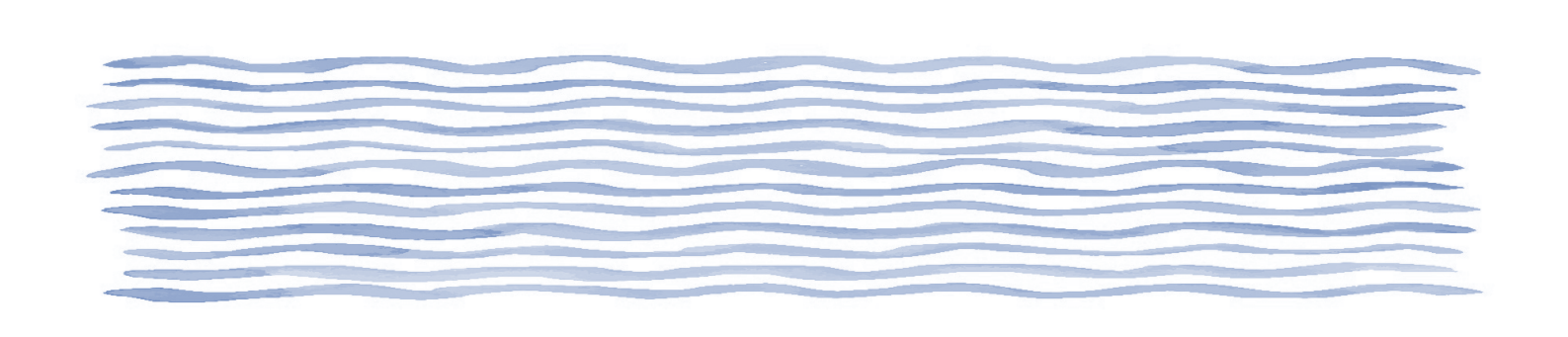


EVALUATION OF FUTURE HYDROLOGICAL SCENARIOS USING STOCHASTIC HIGH-RESOLUTION CLIMATE DATA

P. BURLANDO, N. PELEG, S. MORAGA-NAVARRETE, P. MOLNAR, S. FATICHI



IM AUFTRAG DES BUNDESAMTES FÜR UMWELT BAFU – NOVEMBER 2020

EIN FORSCHUNGSPROJEKT IM RAHMEN DES NCCS THEMENSCHWERPUNKTES "HYDROLOGISCHE GRUNDLAGEN ZUM KLIMAWANDEL" DES NATIONAL CENTRE FOR CLIMATE SERVICES

Impressum

Commissioned by: Federal Office for the Environment (FOEN), Hydrology Division, CH- 3003 Bern. The FOEN is an agency of the Federal Department of the Environment, Transport, Energy and Communications (DETEC)

Contractor: ETH Zürich, Versuchsanstalt für Wasserbau, Hydrologie und Glaziologie (VAW), HIA C58, Hönggerbergring 26, CH-8093 Zürich

Authors: Paolo Burlando⁽¹⁾, Nadav Peleg(1), Jorge Sebastián Moraga-Navarrete (1), Peter Molnar (1) and Simone Fatichi (1,2)

- (1) Institute of Environmental Engineering, ETH Zurich
- (2) Department of Civil and Environmental Engineering, National University of Singapore

FOEN support: Fabia Huesler, Petra Schmocker-Fackel

Note: This study/report was prepared under contract to the Federal Office for the Environment (FOEN). The contractor bears sole responsibility for the content.

Citation: Burlando, P., Peleg, N., Moraga-Navarrete, J.S., Molnar, P., and Fatichi, S. 2020. Evaluation of future hydrological scenarios using stochastic high-resolution climate data. Commissioned by the Federal Office for the Environment (FOEN), Bern, Switzerland. 50 pp, DOI:10.3929/ethz-b-000462637

DOI: 10.3929/ethz-b-000462637

Authors: P. Burlando, N. Peleg, S. Moraga-Navarrete, P.Molnar and S. Fatichi Chair of Hydrology and Water Resources Management, ETH Zurich https://hyd.ifu.ethz.ch

Table of Contents

1	INTRODUCTION	1
2	METHODS	2
_		
	2.1 THE AWE-GEN-2D MODEL	
	2.3 FROM CLIMATE TO HYDROLOGICAL PREDICTIONS	
3	STUDY CATCHMENTS	2
4	DATA	
5	RESULTS	, ,
	5.1 VALIDATION OF AWE-GEN-2D	
	5.2 VALIDATION OF TOPKAPI-ETH	
	5.3 CHANGES IN CLIMATE	
	5.3.1 Domain scale	15
	5.3.2 The 2-km scale	19
	5.4 Changes in Hydrology	21
	5.4.1 Changes of the mean streamflow regime at the catchment outlets (Kl. Emme and Thur)	2
	5.5 Changes to the Mean Inflows into the Reservoirs in the Maggia Basin	
	5.5.1 Changes to extreme flows in the Kl. Emme and Thur	33
6	CONCLUSIONS	37
7	REFERENCES	38

List of Tables

Table 1 – List of ground stations from MeteoSwiss	6
Table 2 – List of climate models from the CH2018 archive that were used in this project	
Table 3 – List of streamflow recording stations that were used in this project.	7

List of Figures

Figure 1 – A schematic representation of the methodological modelling framework. Points 1 to 7 are detailed described in Section 2.3.
Figure 2 – Location map of the catchments. Coordinates are in Swiss projection (CH-1903) in m
Figure 4 – Mean precipitation for the period 1982-2015 as obtained from the RhiresD product (observed) in comparison with the mean ensemble generated by AWE-GEN-2d (simulated)
Figure 6 – A comparison between observed and simulated temperatures for each month. The blue and red solid lines represent the observed and simulated median values (respectively) and the bounded areas represent the observed (blue area) and simulated (dashed lines) 5–95th percentile range (respectively). The observed period covers 34 years of data (1982–2015), while simulations represent the mean of 30 realizations of 30 years each.
Figure 7 – A comparison between observed and simulated precipitation for each month. The blue and red solid lines represent the observed and simulated median values (respectively) and the bounded areas represent the observed (blue area) and simulated (dashed lines) 5–95th percentile range (respectively). The observed period covers 34 years of data (1982–2015), while simulations represent the mean of 30 realizations of 30 years each.
Figure 8 – Validation of annual maximum precipitation intensity at the hourly scale for different return periods in the Kl. Emme (top row) and Thur (bottom row) weather stations. The solid lines represent the observed (blue) and simulated (red) precipitation intensity computed by fitting GEV distribution to the data. The observed period covers 34 years of data (1982–2015), while simulations represent the mean of 30 realizations of 30 years each.
Figure 9 – A comparison between observed and simulated inflow for each month (2006-2015, excluding 2010) in Sambuco reservoir. The blue and red lines represent the observed and simulated mean values (respectively).
Figure 10 – A comparison between observed (blue) and Topkapi-ETH simulated (red) streamflow (outlet of K1. Emme catchment). NSE refers to the Nash–Sutcliffe efficiency that was computed at the hourly scale for the period 2000-2009
Figure 11 – A comparison between observed and simulated streamflow for each month (2000-2009). The blue and red solid lines represent the observed and simulated median values (respectively) and the bounded areas represent the observed (blue area) and simulated (dashed lines) 5–95th percentile range (respectively)
Figure 12 – Comparison between observed and simulated peak-over-threshold at the hourly scale for different return periods in the Kl. Emme (left) Thur (right) catchments. The solid lines represent the observed (blue) and simulated (red) streamflow computed by fitting a Generalized Pareto distribution to the recorded data for the 2000–2009 period. The plotting positions were calculated using Gringorten's equation and the return periods are calculated via the reduced variate method14
Figure 13 – Differences in mean annual temperature between the present period (1976-2005) and future periods for the Kl. Emme, Thur and Maggia catchments. Numbers 1 to 9 refer to the different climate models (see Table 1) and MMM refers to the multi-model mean. Box plots for the present and 1 to 9 simulations represent the stochastic uncertainty for each climate trajectory, and MMM represents the combination of stochastic and climate model uncertainty. Central lines in the box

plots represent the median of the mean annual temperature of the ensemble, while the boxes and	
whisker lines represent the 25-75 th and 5-95 th percentile range of the data. The simulated ensemble	
for each climate trajectory is composed of 30 realizations of 30 years each, bootstrapped from an	
archive of 100 years10	
Figure 14 – Similar plot as Fig. 13, but for the ratios of mean annual precipitation	7
Figure 15 - The ratio between annual maximum precipitation for a given return period of present climate	
(1976-2005) and end of the century climate (2070-2099) at the hourly scale. Numbers 1 to 9 refer to)
the different climate models (see Table 1) and M refers to the multi-model mean. Box plots for the	
present and 1 to 9 represent the stochastic uncertainty for each climate trajectory, and M represents	
the combination of stochastic and climate model uncertainty. Central lines in the box plots represent	t
the median of mean annual maximum precipitation intensity computed from the simulated ensemble	Э
using GEV distribution, while the boxes represent the 5-95th percentile range of the data. The	
simulated ensemble for each climate trajectory is composed of 30 realizations of 30 years each,	
bootstrapped from an archive of 100 years1	8
Figure 16 – Similar plot as Fig. 15, but on a daily scale.	9
Figure 17 – Projected multi-model mean anomalies in climate variables relative to the present climate	
(1976–2005) in the Kl. Emme (a-d), Thur (e-h) and Maggia (i-l). Panels (a, e), (c, g) and (i, k) show	V
the monthly precipitation and temperature anomalies for each future period, respectively, whereas	
panels (b, f), (d, h) and (j, l) show the spatial distribution of the annual anomaly by the end of the	
century (2080–2089)20	0
Figure 18 – Differences in the temperature of the hottest day in the year (annual maximum of daily T_{max} ,	
TXx) and ration change of mean daily rainfall (MEA) between the present climate (1976-2005) and	
end of the century scenarios (2070-2099, multi-model mean)	1
Figure 19 – Differences in mean annual streamflow between the present and future periods for the Kl.	
Emme and Thur catchments. Numbers 1 to 9 refer to the different climate models and M refer to the	•
multi-model mean. Box plots for the present and 1 to 9 represent the stochastic uncertainty for each	
climate trajectory, and M represents the combination of stochastic and climate model uncertainty.	
Central lines in the box plots represent the median of mean annual streamflow of the ensemble,	
while the boxes and whisker lines represent the 25-75th and 5-95th percentile range of the data. The	•
simulated ensemble for each climate trajectory is composed of 30 realizations of 30 years each,	
bootstrapped from an archive of 100 years	2
Figure 20 – The ratio between monthly streamflow of present (1976-2005, grey), early-mid-century	
(2020-2049, blue), mid-century (2040-2079, red) and end of the century (2070-2099, yellow)	
periods. Box plots for the present period represent the stochastic uncertainty for the future periods	
represent the combination of stochastic and climate model uncertainty. Central lines in the box plots	S
represent the median of mean monthly streamflow computed from the simulated ensemble, while	
the boxes represent the 5-95th percentile range of the data. The simulated ensemble for each climate	
trajectory is composed of 30 realizations of 30 years each, bootstrapped from an archive of 100	
years	3
Figure 21 – Change in mean effective saturation (a, b), snow water equivalent (c, d) and annual	
evapotranspiration (e, f) for the Kl. Emme and Thur catchments. All values correspond to the	
averages of the multi-model-mean (MMM) at the end of the century (2080-2089) minus the present	t
climate condition2	4
Figure 22 – Differences in snow water equivalent (SWE) between the present and future periods for the	
Kl. Emme and Thur catchments. Numbers 1 to 9 refer to the different climate models and M refer to)
the multi-model mean. Box plots for the present and 1 to 9 represent the stochastic uncertainty for	
each climate trajectory, and M represents the combination of stochastic and climate model	
uncertainty. Central lines in the box plots represent the median of mean SWE of the ensemble, while	۵

simulated	and whisker lines represent the 25-75th and 5-95th percentile range of the data. The ensemble for each climate trajectory is composed of 30 realizations of 30 years each,
	ped from an archive of 100 years
	erage snow height in the Kl. Emme catchment for the present period (left) and end of the left, multi-model-mean)
• .	nthly streamflow (thick black line) and its hydrological components at the outlet of the K1.
Emme (a towards t	c) and Thur (b, d) river catchments for the present climate (a, b) and the changes projected to end of the century (2080–2089, c, d). The bars corresponding to evapotranspiration an increase in soil water volume (pink) are depicted as negative contributions to the water
	tial distribution of 96 sub-catchments in the Kl. Emme river network (a) and 140 of the
Thur rive	network (b). River reaches are drawn according to their Strahler order and markers are based on their average specific annual discharge in the present climate27
	pacts on streamflow in 97 Kl. Emme river sub-catchments (a, c, e) and 140 Thur river sub-
catchmen	s (b, d, f). The change rates between the present climate and the end of the century are
7-day mis	for each river section are shown for the maximum hourly flow (a, b), mean flow (c, d) and imum flow (e, f). The markers in all plots are colored according to the mean specific v in the present climate, and the river section corresponding to the outlet of the entire
	is highlighted with a black border
-	er network under present (circles) and future (triangles) climate conditions29
	nilar to Fig. 27, but for the Thur river basin
Figure 29 – Sc	nematic representation of the hydro-power reservoirs in the Maggia river basin. Image is MA website ¹ 31
Numbers for the pr represent plots repr lines repr climate to	ferences in mean annual inflow to the reservoirs between the present and future periods. It to 9 refer to the different climate models and M refer to the multi-model mean. Box plots sent and 1 to 9 represent the stochastic uncertainty for each climate trajectory, and M the combination of stochastic and climate model uncertainty. Central lines in the box esent the median of mean annual streamflow of the ensemble, while the boxes and whisker sent the 25-75th and 5-95th percentile range of the data. The simulated ensemble for each ajectory is composed of 30 realizations of 30 years each, bootstrapped from an archive of
mid centry yellow) periods rebox plots ensemble	e ratio between monthly inflow into the reservoirs of the present (1976-2005, grey), early-ry (2020-2049, blue), mid-century (2040-2079, red) and end of the century (2070-2099, criods. Box plots for the present period represent the stochastic uncertainty for the future present the combination of stochastic and climate model uncertainty. Central lines in the represent the median of mean monthly streamflow computed from the simulated while the boxes represent the 5-95 th percentile range of the data. The simulated ensemble limate trajectory is composed of 30 realizations of 30 years each, bootstrapped from an 100 years.
-	e ratio between annual maximum streamflow for a given return period of present climate
the differ 9 represe of stocha mean ann	(5) and end of the century climate (2070-2099) at the hourly scale. Numbers 1 to 9 refer to an climate models and M refer to the multi-model mean. Box plots for the present and 1 to the stochastic uncertainty for each climate trajectory, and M represents the combination tic and climate model uncertainty. Central lines in the box plots represent the median of the maximum streamflow computed from the simulated ensemble using GEV distribution, boxes represent the 5-95th percentile range of the data. The simulated ensemble for each

climate trajectory is composed of 30 realizations of 30 years each, bootstrapped from an archive of	f
100 years	.35
Figure 33 – Similar plot as Fig. 22, but on a daily scale.	.35
Figure 34 – Monthly frequency of the hourly (a, c) and daily (b, d) maximum yearly outlet streamflow	
occurring in each month in the K1. Emme (a-b) and Thur (c-d) rivers	.36
Figure 35 – Similar plot as Fig. 22, but for NM7Q. Note that for the GEV calculation the minimum	
annual streamflow was multiple by -1	.36

Summary

The present report illustrates the outcomes of a project aimed to analyse the detailed and spatiotemporal highly-resolved impact of climate change on the hydrological response of three catchments in Switzerland, Thur, Kl. Emme and Maggia.

This project is part of the NCCS efforts to explore climate change impacts on hydrology in Switzerland and is unique in three aspects. First, it allows for the first time the investigation of climate impacts on the hydrology at sub-daily (hourly) scales; second, it enables exploring the effects of the natural (stochastic) climate variability on the hydrological components, thus allowing better estimation of the expected uncertainty in future hydrological predictions; and third, it allows the detailed exploration of the changes affecting the hydrological components within the catchments also exploring them at the grid cell or sub-catchment scales. To that end, high temporal and spatial resolution gridded climate variables, characterised by hourly and hundreds of meters scales, i.e. much finer resolution than that of the MeteoSwiss CH2018 official scenarios, were stochastically simulated using the advanced state-of-the-art AWE-GEN-2d weather generator model to form ensembles representing the future climate for the highest greenhouse-gasses emission scenario (RCP8.5). The fully distributed physically-based hydrological model Topkapi-ETH, capable of simulating streamflow and the other land components of hydrological processes over complex terrain, was used to estimate the changes affecting the key hydrological components in space and time.

The projected changes in temperatures are characterized by high uncertainty. The temperatures in the K1. Emme and Thur catchments are projected to increase in a range of 0.4-2 °C, 1.4-3 °C and 2.7-5.3 °C when comparing the periods of 2020-2049, 2040-2069 and 2070-2099 (respectively) to the present climate (1976-2005). A higher increase in temperatures is projected in the Maggia catchment, in the order of 3.4-6 °C for the end of the century. Model results suggest a spatially uniform increase in temperature over the catchments.

The magnitude and spatial patterns of change in precipitation differ between catchments. While in the K1. Emme and Maggia catchments a general decrease in precipitation is predicted, an increase in precipitation is projected in the Thur catchment. The decrease in precipitation in the K1. Emme and Maggia catchments is associated with high uncertainties: -15% to +3%, -18% to +6%and -17% to +8% for the periods 2020-2049, 2040-2069 and 2070-2099 (respectively) in comparison to the period of 1976-2005. The change in precipitation considerably overlapped with the present natural precipitation variability that is in the order of $\pm 5\%$. The increase in precipitation in the Thur catchment exceeds the present natural precipitation variability. The change is projected in the range of +6% to +33%, +9% to +34% and +14% to +40% for the same periods as mentioned above. In the Kl. Emme and Thur catchments, precipitation tends to decrease in future climate over the mountainous regions and increase in the low elevation areas, while in the Maggia catchment precipitation is generally decreasing, with a higher magnitude of decrease over the mountainous areas in comparison to the lower areas. Extreme rainfall intensities at the hourly scale are characterized with high natural variability, in the order of $\pm 10\%$ for the 2-year return period and $\pm 30\%$ for the 30-year return period in all catchments. The uncertainty in the change of extreme rainfall intensity is in the same order of magnitude as the natural variability and largely overlap with it, thus making the detection of clear trends difficult.

Climate change is predicted to affect the hydrological components in the catchments. The notable changes are a meaningful decrease in snowmelt during spring – snowmelt contribution to the streamflow is expected to decrease by 50% (for both catchments) at the end of the century – and an increase in summer evapotranspiration in the order of 10%. Model results indicate a decrease in mean annual streamflow for the Kl. Emme and Thur catchments in future climates – up to - 23% in comparison to the present – with the most meaningful change already occurring in the period 2020-2049. However, the uncertainty in future streamflow predictions is high, with some climate models forcing an increase in streamflow up to 5% and 12% for the Kl. Emme and Thur catchments, respectively. For both catchments, winter flows are predicted to increase and summer flows are predicted to decrease, with magnitudes and uncertainties increasing toward the end of the century. In the Maggia, spatially different responses to climate change were detected – e.g. a decrease in inflows was found to the large reservoirs (e.g. Sambuco), while small reservoirs could experience an increase in inflows.

In terms of changes to streamflow extremes, no changes in the statistics of maximum annual streamflow at the hourly scale were identified for the high-frequency (2-year return period) flows in the Kl. Emme and Thur catchments. For lower frequency hourly annual maximum flows (i.e. 30-year return period) it is impossible to identify a clear change signal as the uncertainty in the change is very high (-40% to +60%) and largely matches the stochastic variability of present-day climate. Most models, however, agree on a reduction in low-flows statistics in the Kl. Emme and Thur catchments, where a median reduction of 25% is foreseen for the 7-day low-flows statistics at the end of the century. Moreover, all downscaled climate trajectories agree that hourly streamflow extremes will become less frequent during summer – remaining this season the main period of flood occurrences – and more frequent during winter.

Zusammenfassung

Der vorliegende Bericht veranschaulicht die Ergebnisse eines Projekts, das darauf abzielte, die detaillierten und räumlich-zeitlich hoch aufgelösten Auswirkungen des Klimawandels auf die hydrologische Reaktion von drei Einzugsgebieten in der Schweiz, Thur, Kl. Emme und Maggia zu analysieren.

Dieses Projekt ist Teil der NCCS-Bemühungen zur Erforschung der Auswirkungen des Klimawandels auf die Gewässersysteme in der Schweiz und ist in dreierlei Hinsicht einzigartig. Erstens ermöglicht es zum ersten Mal die Untersuchung der Klimaauswirkungen auf die Gewässersysteme auf untertägiger (stündlicher) Skala; zweitens ermöglicht es die Erforschung der Auswirkungen der natürlichen (stochastischen) Klimavariabilität auf die hydrologischen Komponenten, was eine bessere Abschätzung der erwarteten Unsicherheit in zukünftigen hydrologischen Vorhersagen ermöglicht; und drittens ermöglicht es die detaillierte Erforschung der Veränderungen, die die hydrologischen Komponenten innerhalb der Einzugsgebiete betreffen, auch auf der Skala der Rasterzellen oder Untereinzugsgebiete. Zu diesem Zweck wurden zeitlich und räumlich hoch aufgelöste gerasterte Klimavariablen, die sich durch stündliche und Hunderte von Metern Skalen auszeichnen, d.h. eine viel feinere Auflösung als die der offiziellen CH2018-Szenarien von MeteoSwiss, stochastisch mit dem hochmodernen AWE-GEN-2d Wettergeneratormodell simuliert, um Ensembles zu bilden, die das zukünftige Klima für das höchste Treibhausgas-Emissionsszenario (RCP8.5) abbilden. Das vollständig ausgebaute, physikalisch basierte hydrologische Modell Topkapi-ETH, das in der Lage ist, den Flusslauf und die anderen Landkomponenten der hydrologischen Prozesse in komplexem Gelände zu simulieren, wurde verwendet, um die Änderungen abzuschätzen, die die wichtigsten hydrologischen Komponenten in Raum und Zeit betreffen.

Die projizierten Änderungen der Temperaturen sind durch hohe Unsicherheiten gekennzeichnet. Die Temperaturen in den Einzugsgebieten Kl. Emme und Thur werden in einem Bereich von 0,4-2 °C, 1,4-3 °C und 2,7-5,3 °C ansteigen, wenn man die Zeiträume 2020-2049, 2040-2069 und 2070-2099 (jeweils) mit dem heutigen Klima (1976-2005) vergleicht. Im Maggia-Einzugsgebiet wird ein höherer Temperaturanstieg prognostiziert, in der Grössenordnung von 3,4-6 °C für das Ende des Jahrhunderts. Die Modellergebnisse deuten auf einen räumlich gleichmässigen Temperaturanstieg in den Einzugsgebieten hin.

Das Ausmass und die räumlichen Muster der Niederschlagsänderung unterscheiden sich zwischen den Einzugsgebieten. In den Einzugsgebieten K1. Emme und Maggia wird eine generelle Abnahme des Niederschlags vorhergesagt, wohingegen im Einzugsgebiet Thur eine Zunahme des Niederschlags erwartet wird. Die Abnahme des Niederschlags in den Einzugsgebieten K1. Emme und Maggia ist mit hohen Unsicherheiten verbunden: -15% bis +3%, -18% bis +6% und -17% bis +8% für die Perioden 2020-2049, 2040-2069 und 2070-2099 (jeweils) im Vergleich zur Periode 1976-2005. Die Änderung des Niederschlags überschneidet sich erheblich mit der gegenwärtigen natürlichen Niederschlagsvariabilität, die in der Grössenordnung von ±5% liegt. Die Niederschlagszunahme im Einzugsgebiet Thur übersteigt die derzeitige natürliche Niederschlagsvariabilität. Die Änderung wird im Bereich von +6% bis +33%, +9% bis +34% und +14% bis +40% für die gleichen Zeiträume wie oben erwähnt prognostiziert. In den Einzugsgebieten K1. Emme und Thur nimmt der Niederschlag im zukünftigen Klima über den

Gebirgsregionen tendenziell ab und in den tiefer gelegenen Gebieten zu, wohingegen im Einzugsgebiet der Maggia der Niederschlag generell abnimmt, wobei die Abnahme über den Gebirgsregionen im Vergleich zu den tiefer gelegenen Gebieten stärker ausfällt. Extreme Niederschlagsintensitäten auf der stündlichen Skala sind durch eine hohe natürliche Variabilität gekennzeichnet, in der Grössenordnung von $\pm 10\%$ für die 2-jährige Wiederkehrperiode und $\pm 30\%$ für die 30-jährige Wiederkehrperiode in allen Einzugsgebieten. Die Unsicherheit in der Veränderung der extremen Niederschlagsintensität liegt in der gleichen Grössenordnung wie die natürliche Variabilität und überschneidet sich weitgehend mit ihr, was die Erkennung eindeutiger Trends erschwert.

Es wird vorhergesagt, dass der Klimawandel die hydrologischen Komponenten in den Einzugsgebieten beeinflussen wird. Die bemerkenswerten Änderungen sind ein deutlicher Rückgang der Schneeschmelze im Frühjahr – der Beitrag der Schneeschmelze zum Abfluss des Flusses wird bis zum Ende des Jahrhunderts voraussichtlich um 50% (für beide Einzugsgebiete) abnehmen – und ein Anstieg der Verdunstung im Sommer in der Grössenordnung von 10%. Die Modellergebnisse zeigen eine Abnahme des mittleren jährlichen Abflusses für die Einzugsgebiete Kl. Emme und Thur in zukünftigen Klimaten – bis zu -23% im Vergleich zu heute – wobei die bedeutendste Änderung bereits in der Periode 2020-2049 auftritt. Allerdings ist die Unsicherheit in den zukünftigen Abflussvorhersagen hoch, wobei einige Klimamodelle einen Anstieg des Abflusses um bis zu 5% und 12% jeweils für die Einzugsgebiete Kl. Emme und Thur vorhersagen. Für beide Einzugsgebiete wird eine Zunahme der Winterabflüsse und eine Abnahme der Sommerabflüsse vorhergesagt, wobei die Grössenordnungen und Unsicherheiten gegen Ende des Jahrhunderts zunehmen. In Maggia wurden räumlich unterschiedliche Reaktionen auf den Klimawandel festgestellt – z.B. wurde eine Abnahme der Zuflüsse zu den grossen Stauseen (z.B. Sambuco) festgestellt, wohingegen kleine Stauseen eine Zunahme der Zuflüsse erfahren konnten.

In Bezug auf Änderungen der Abflussextreme wurden keine Änderungen in der Statistik der maximalen jährlichen Abflüsse auf der Stundenskala für die hochfrequenten (2-jährige Wiederkehrperiode) Abflüsse in den Einzugsgebieten Kl. Emme und Thur festgestellt. Für die niederfrequenten stündlichen jährlichen Maximalabflüsse (d.h. 30-jährige Wiederkehrperiode) ist es unmöglich, ein klares Änderungssignal zu identifizieren, da die Unsicherheit der Änderung sehr hoch ist (-40% bis +60%) und weitgehend mit der stochastischen Variabilität des heutigen Klimas übereinstimmt. Die meisten Modelle stimmen jedoch überein, dass die Niedrigwasserzahlen in den Einzugsgebieten von Kl. Emme und Thur abnehmen werden, wobei für die 7-tägigen Niedrigwasserzahlen am Ende des Jahrhunderts eine mittlere Abnahme von 25 % vorhergesagt wird. Darüber hinaus stimmen alle herunterskalierten Klimaprognosen darin überein, dass stündliche Abflussextreme im Sommer seltener werden – diese Jahreszeit bleibt die Hauptperiode für Hochwasserereignisse – und im Winter häufiger auftreten werden.

Résumé

Le présent rapport illustre les résultats d'un projet visant à analyser l'impact détaillé et à haute résolution spatio-temporelle du changement climatique sur la réponse hydrologique de trois bassins versants en Suisse, de la Thur, la Petite Emme et la Maggia.

Ce projet fait partie des efforts du NCCS pour étudier les impacts du changement climatique sur l'hydrologie en Suisse et est unique en trois aspects. Premièrement, il permet pour la première fois l'étude d'impacts climatiques sur l'hydrologie à des échelles sous-quotidiennes (horaires) ; deuxièmement, il permet d'étudier les effets de la variabilité climatique (stochastique) naturelle sur les composants hydrologiques, permettant ainsi une meilleure estimation de l'incertitude attendue dans de futures prévisions hydrologiques ; et troisièmement, il permet l'exploration détaillée des changements affectant les composants hydrologiques dans les bassins versants, les explorant aussi à l'échelle de cellules de grille ou de sous-bassins versants. À cette fin, des variables climatiques grillées à haute résolution temporelle et spatiale, caractérisées par des échelles horaires et de centaines de mètres, c'est-à-dire une résolution bien plus fine que celle des scenarios officiels CH2018 de MeteoSwiss, ont été simulées de manière stochastique en utilisant le modèle de pointe de génération de données météorologiques AWE-GEN-2d pour former des ensembles représentant le climat futur pour le scenario des émissions de gaz à effet de serre les plus élevées (RCP8.5). Le modèle hydrologique Topkapi-ETH entièrement distribué basé sur la physique, capable de simuler l'écoulement fluvial et les autres composants terrestres de processus hydrologiques sur des terrains complexes, a été utilisé pour estimer les changements affectant les composants hydrologiques clé dans l'espace et le temps.

Les changements projetés de température sont caractérisés par une incertitude élevée. Les températures dans les bassins versants de la Petite Emme et de la Thur sont prévues d'augmenter dans une plage de 0,4 à 2 °C, 1,4 à 3 °C et 2,7 à 5,3 °C lors de la comparaison des périodes 2020-2049, 2040-2069 et 2070-2099 (respectivement) au climat actuel (1976-2005). Une augmentation plus importante des températures est prévue dans le bassin versant de la Maggia, de l'ordre de 3,4 à 6 °C pour la fin du siècle. Les résultats de modèles suggèrent une augmentation spatialement uniforme des températures le long des bassins versants.

L'ampleur et les modèles spatiaux des changements dans les précipitations varient entre les bassins versants. Alors qu'une réduction générale des précipitations est prédite dans les bassins versants de la Petite Emme et de la Maggia, une augmentation des précipitations est prévue dans le bassin versant de la Thur. La réduction des précipitations dans les bassins versants de la Petite Emme et de la Maggia est associée à des incertitudes élevées: -15% à +3%, -18% à +6% et -17% à +8% pour les périodes de 2020-2049, 2040-2069 et 2070-2099 (respectivement), par rapport à la période de 1976-2005. Le changement dans les précipitations s'est recoupé fortement avec la variabilité naturelle actuelle des précipitations, qui est de l'ordre de ±5%. L'augmentation des précipitations dans le bassin versant de la Thur dépasse la variabilité naturelle actuelle des précipitations. Le changement est prévu être dans la plage de +6% à +33%, +9% à +34% et +14% à +40% pour les mêmes périodes que celles mentionnées ci-dessus. Dans les bassins versants de la Petite Emme et de la Thur, les précipitations tendent à diminuer, dans le climat futur, le long des régions montagneuses et à augmenter dans les zones de basse altitude, tandis que dans le bassin versant de la Maggia, les précipitations diminuent en règle générale, avec une réduction d'un

ordre de grandeur supérieur le long des régions montagneuses par rapport aux zones plus basses. Les intensités des précipitations extrêmes à l'échelle horaire sont caractérisées par une variabilité naturelle élevée, de l'ordre de $\pm 10\%$ pour la période de retour de 2 ans et de $\pm 30\%$ pour la période de retour de 30 ans dans tous les bassins versants. L'incertitude dans le changement de l'intensité des précipitations extrême est du même ordre de grandeur que la variabilité naturelle et se recoupe fortement avec celle-ci, rendant la détection de tendances claires difficile.

Il est prévu que le changement climatique affectera les composants hydrologiques dans les bassins versants. Les changements notables sont une diminution importante de la fonte des neiges au printemps – la contribution de la fonte des neiges au débit devrait diminuer de 50% (pour les deux bassins versants) à la fin du siècle – et une augmentation de l'évapotranspiration estivale de l'ordre de 10%. Les résultats de modèle indiquent une diminution du débit annuel moyen pour les bassins versants de la Petite Emme et de la Thur dans des climats futurs, jusqu'a -23% par rapport au débit actuel, le changement le plus important se produisant déjà dans la période de 2020-2049. Cependant, l'incertitude des prévisions de débits futurs est élevée, certains modèles climatiques forçant une augmentation du débit jusqu'a 5% et 12% pour les bassins versants de la Petite Emme et de la Thur, respectivement. Pour les deux bassins versants, on prévoit que les débits hivernaux augmenteront et que les débits estivaux diminueront, avec des grandeurs et des incertitudes croissantes vers la fin du siècle. Dans la Maggia, des réponses au changement climatique spatialement différentes ont été détectées, p. ex. une réduction des débits entrants aux grands réservoirs (p. ex. Sambuco) a été détectée, tandis que les petits réservoirs pourraient être soumis à une augmentation des débits entrants.

En termes de changements des valeurs extrêmes de débit, aucun changement n'a été identifié dans les statistiques de débits annuels maximaux à l'échelle horaire pour les débits haute fréquence (période de retour de 2 ans) dans les bassins versants de la Petite Emme et de la Thur. Pour les débits maximaux annuels de fréquence plus basse (c'est-à-dire d'une période de retour de 30 ans), il est impossible d'identifier un signal de changement clair, étant donné que l'incertitude liée au changement est très élevée (-40% à +60%) et concorde en grande partie avec la variabilité stochastique du climat actuel. La plupart des modèles, cependant, s'accordent sur une réduction dans les statistiques des étiages dans les bassins versants de la Petite Emme et de la Thur, pour lesquels une réduction moyenne de 25% est prévue pour les statistiques des étiages de 7 jours à la fin du siècle. En outre, toutes les trajectoires climatiques à échelle réduite conviennent que les valeurs extrêmes de débit horaires deviendront moins fréquentes durant l'été, cette saison restant la période principale d'inondations, et plus fréquentes durant l'hiver.

EVALUATION OF FUTURE HYDROLOGICAL SCENARIOS USING STOCHASTIC HIGH-RESOLUTION CLIMATE DATA

EVALUATION OF FUTURE HYDROLOGICAL SCENARIOS USING STOCHASTIC HIGH-RESOLUTION CLIMATE DATA

1 INTRODUCTION

New climate change scenarios for Switzerland were released in 2018 (CH2018, 2018). They replaced the Swiss national climate scenarios projections that were introduced in 2011 (CH2011, 2011). The new CH2018 scenarios are based on the latest set of European climate model simulations from the Coordinated Regional Climate Downscaling Experiment (EURO-CORDEX). An assessment of the impacts of the CH2011 climate scenarios on the hydrology regime was conducted and summarized in a report that was published by various Swiss Federal agencies and research institutes (CH-Impacts, 2014). With the availability of the new climate scenarios, a need emerges of producing a new assessment of the impact of climate change on the hydrology. Previous studies focused essentially on average changes to the hydrological components at daily scale (e.g. Addor et al., 2014). New numerical models and stochastic-statistical tools that were introduced in recent years allow today the analyses of climate impacts on the hydrology at finer, subdaily scales (e.g. Fatichi et al., 2015; Fatichi et al., 2016b; Peleg et al., 2017). Moving toward climatic and hydrological simulations at, e.g. hourly scales reduces uncertainties in hydrological model predictions and enable exploring changes to essential hydrological components, such as hourly streamflow peaks, which otherwise remain masked by the space-time aggregated nature of the predictions (e.g. Ragettli et al., 2014). Moreover, in the previous assessments of the climate change impacts on the hydrology, only two uncertainties that are related to climate, namely - the uncertainties emerging from the emission scenarios and various climate models, were considered. Recently it was shown that the internal (stochastic) climate variability, also known as natural climate variability (Deser et al., 2012), can contribute significantly to the total uncertainty emerging from climate (Fatichi et al., 2016a; Fatichi et al., 2014; Peleg et al., 2019). This implies that methods used to simulate the future climate and hydrological response should be able to account for high temporal (sub-daily scale) and spatial (sub-kilometre scale) resolution and for the stochastic climatic component.

In this project, we used state-of-the-art numerical models and methods to reveal the impacts of changes in climate on hydrological components that were so far "hidden" due to the coarse resolution in time and space that characterised the past climate impacts studies. In our study, we also explicitly computed the stochastic uncertainty of climate, in order to provide a sounder estimation of the projected hydrological uncertainties. The project aims at complementing and extending the existing studies by approaching the problem of future hydrological scenarios through the highest level of model sophistication, though addressing changes predicted across the entire basin scale. The changes in climate and hydrological components were investigated for three catchments located in different areas in Switzerland (Thur, Kl. Emme and Maggia). The ultimate goal of this project is to provide predictions of the key hydrological variables that characterize the hydrological response (e.g. streamflow, evapotranspiration, soil wetness, snowmelt contribution and extremes) in selected but representative catchments, while considering the climate uncertainty due to internal climate variability for a median climate trajectory (as simulated by the climate models considered by the CH2018 scenarios) up to the end of the 21st century.

2 METHODS

The general methodological framework of this project is illustrated in Figure 1. This illustrates the workflow that makes use of two state-of-the-art models, a high-resolution stochastic weather generator (AWE-GEN-2d) and a fully distributed hydrological model (Topkapi-ETH). AWE-GEN-2d was used to generate climate ensembles for the present and the future climate forced with the RCP8.5 emission scenario. Topkapi-ETH was used to estimate the changes in the future hydrological regimes and the associated uncertainties. The models and the details of the procedures that were applied are described in the following sections.

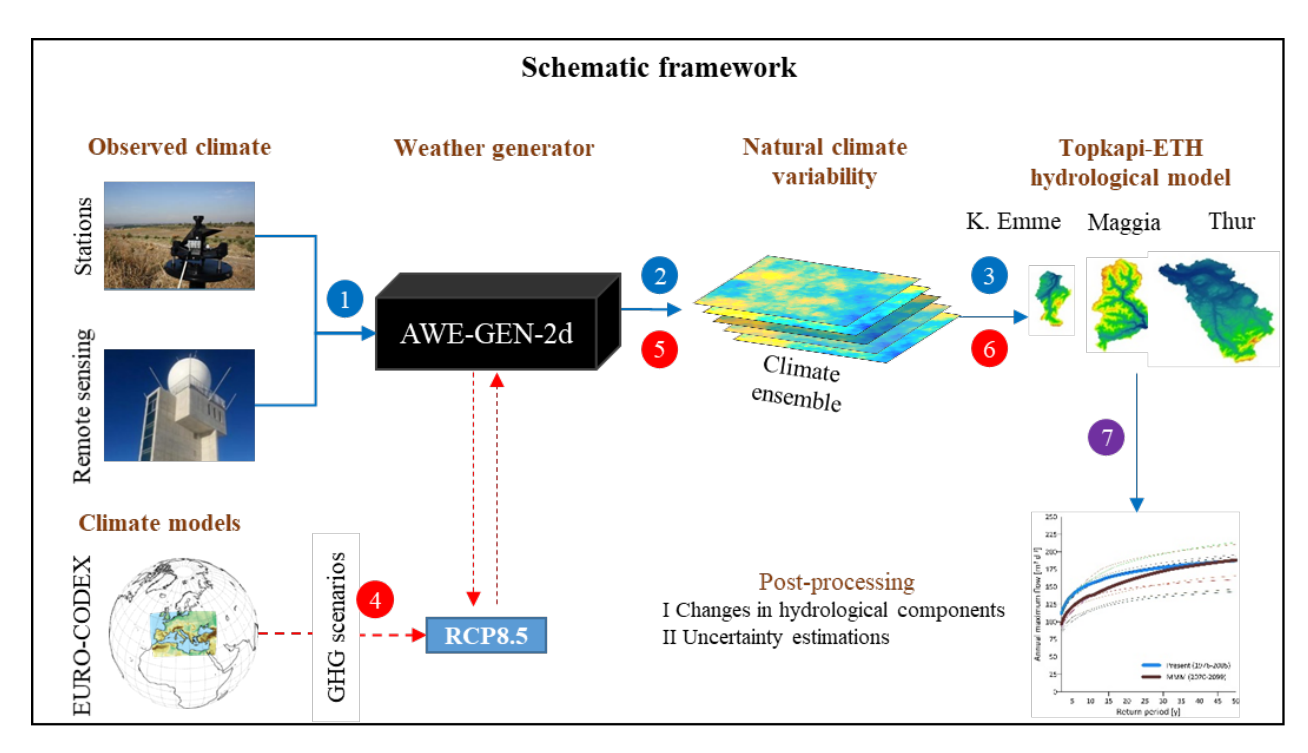


Figure 1 – A schematic representation of the methodological modelling framework. Points 1 to 7 are detailed described in Section 2.3.

2.1 THE AWE-GEN-2D MODEL

Weather generators (WGs) are numerical tools designed to produce synthetic time series of various meteorological variables of theoretically infinite length for a given climate and location. Most of the existing WGs are designed for station-scale applications or as multi-station generators and simulate climate variables at a daily or coarser temporal resolution (e.g. Keller et al., 2015). Gridded stochastic WGs are a suitable tool to generate multiple realizations of different climate variables at high spatial and temporal resolution while reproducing the spatial climate variability and the natural climate variability. Recently, a new stochastic weather generator model, the AWE-GEN-2d (*Advanced WEather GENerator for a 2-dimensional grid*), was presented by Peleg et al. (2017). The model combines physical and stochastic approaches to simulate key climate variables at high spatial and temporal resolution: 2 km x 2 km and 1 h for precipitation and cloud cover and 100 m x 100 m and 1 h for near-surface air temperature, solar

radiation, vapor pressure, atmospheric pressure, and near-surface wind. The climate variables are auto- and cross-correlated in time and space. The WG is relatively parsimonious in terms of computational demand and allows the generation of multiple stochastic realizations in a fast and efficient way. Its performance was tested for small areas with a complex topography (Peleg et al., 2017, 2019; Skinner et al., 2020), as well as for larger domains (Peleg et al., 2020). The high-resolution climate variables reproduced by the WG can serve as inputs into distributed hydrological models. Moreover, AWE-GEN-2d is particularly suitable for studies where exploring climate forcing uncertainty at multiple spatial and temporal scales is fundamental as the WG can be conveniently reparametrized to simulate different climates (Peleg et al., 2019).

2.2 TOPKAPI-ETH HYDROLOGICAL MODEL

A distributed investigation of the propagation of climate change effects on streamflow at fine spatial and temporal scales requires the use of a fully distributed hydrological model. The Topkapi-ETH model (Fatichi et al., 2015) used in this study is an advanced version of the TOpographic Kinematic APproximation and Integration model (Topkapi; Todini and Ciarapica, 2001, Ciarapica and Todini, 2002). Among other applications, the model was used to investigate climate change effects on the hydrology of the Po and Rhone river basins (Fatichi et al., 2014, Fatichi et al. 2015), and of the Kl. Emme (Battista et al., 2020; Paschalis et al., 2014). The model uses a grid-based representation of topography and a vertical discretization of the subsurface in three layers. The first two layers represent shallow and deep soil horizons and are schematized as non-linear reservoirs following the integration of the kinematic approximation of the momentum and mass conservation equations, whereas the third layer is schematized as a linear reservoir useful to mimic the behaviour of slow-flow components such as porous or fractured rock aquifers. Grid elements are connected in the surface and the subsurface according to topographic gradients. The model simulates surface and subsurface flow while considering processes as interception, infiltration, evapotranspiration, and snow and ice melt over each grid cell. Topkapi-ETH represents a reasonable compromise between the fully physically-based meaningful representation of hydrological processes and computational time for large scales (>1,000 km²), long-term (>20 y), high-resolution (<1 km², hourly) distributed simulations in a stochastic framework. In the context of this study it is worth to mention that it can preserve relatively high-resolution topography, which is an important asset for hydrological simulations in complex terrain.

2.3 From Climate to Hydrological Predictions

The methodological modelling framework of this study required to carry out seven steps, illustrated in Fig. 1, to estimate the changes in the hydrological components for the future climate. First, the AWE-GEN-2d model was used to simulate the ensembles of climate variables representing the present climate (steps 1 and 2). Three ensembles were generated, one for each of the examined catchments. The methods for calibrating and validating the AWE-GEN-2d model are described in detail by Peleg et al. (2017). In step 1, data that were obtained from different sources (see Section 4) were analysed and processed to be used as input variables for the model. In step 2, the climate ensembles representing the present period (1976-2005) were generated. Each ensemble is composed of 30 realizations and each realization is composed of 30 members (years). In total 2,700 years were simulated (3 x 30 x 30; #catchment-ensembles, #realizations, #members). Note that for the calibration and evaluation phases we assume that the observed data

are stationary, i.e. no climate trends exist. The following climate variables were simulated: precipitation, cloud cover, near-surface air temperature, relative humidity, and solar radiation. All variables were simulated over a grid, with a temporal resolution of 1 h and a spatial resolution of 2 km x 2 km.

The Topkapi-ETH model was calibrated for the three catchments using observed data of climate (precipitation, temperature and cloud cover) and streamflow (see Section 4). The model was calibrated following a well-established calibration procedure that was used in past studies for various catchments in Switzerland (e.g. Fatichi et al., 2015; Pappas et al., 2015; Paschalis et al., 2014). After calibration, the present climate ensembles, simulated in steps 1 and 2, were used as input into Topkapi-ETH to simulate the hydrological flows at present climate conditions (step 3). The simulated streamflow with AWE-GEN-2d data was compared with the observed streamflow to evaluate both models (AWE-GEN-2d and Topkapi-ETH) abilities in statistically reproducing the hydrology for the present climate.

Next, the AWE-GEN-2d model was re-parameterised to simulate climate ensembles for future climate conditions. To that end, 9 regional climate models (Section 4) from the EURO-CORDEX project (quantile mapped following Rajczak et al. (2016) method as in CH2018), which simulate the future climate for the highest emission scenario path (RCP8.5), were used. The parameters used to simulate precipitation and temperature in AWE-GEN-2d for the present climate were re-calibrated (step 4) to follow the statistics of the future climate by applying a factor of change method on a seasonal basis (e.g. Fatichi et al., 2011). Future climate ensembles were then generated for each of the catchments (step 5). A 30-year 'moving window' technique was used to generate continuous precipitation and temperature series for the period between 2020 and 2099 (Peleg et al., 2019). The ensembles generated for the future climate consist of 10 realizations of 10 years each, for each decade and regional climate model. In total 21,600 years were simulated (3 x 9 x 10 x 10 x 8; #catchment-ensemble, #climate-models, #realizations, #members, #decades). The future climate ensembles were then used as input into Topkapi-ETH to simulate the hydrological flows for the future (step 6).

Last, the impacts of climate change on the hydrology were examined (step 7). The post-processing stage includes an assessment of the median and variability changes in the hydrological regime that were projected for each of the catchments and each of the climate trajectories (i.e. for each climate model). The stochastic variability was quantified by the 5-95th percentile range of the simulated, either climatic or hydrological, variable (as in Peleg et al., 2017, 2019). In addition to the stochastic uncertainty, the hydrological uncertainty emerging from the various regional climate models was computed. To obtain a detailed analysis of the impact on the hydrological processes, we analysed the changes in seasonal streamflow, annual high and low flows, evapotranspiration, soil moisture and flow contribution from snow/ice melt.

3 STUDY CATCHMENTS

Three catchments representative of basin characteristics frequently found in Switzerland were chosen for this project: the Thur, Maggia and Kl. Emme (Figure 2). The catchments are characterised by a very heterogeneous spatial precipitation distribution, complex terrain and different size. The rationale for their selection was to favour catchments with minimum anthropogenic

influences, in the cases of Kl. Emme and Thur, and with a high degree of impounding for hydropower production, in the case of Maggia.

Thur catchment. The catchment is located in the north-eastern part of Switzerland (latitude, 47.4° N, longitude, 9.1° E, at catchment centre-point). It is a tributary of the Rhine, with a total drained area of 1,730 km² and an elevation range between 359 and 2,434 m and mean elevation of 773 m. Precipitation averaged over the entire catchment for the present climate is 1,350 mm y⁻¹. There are neither reservoirs nor lakes in the catchment.

Maggia catchment. The catchment is located in the southern part of Switzerland (46.3° N, 8.6° E), and a small part of it belongs to Italy. It outflows into Lago Maggiore, with a total drained area of 840 km² and an elevation range between 204 and 3,208 m with a mean of 1,532 m. Precipitation averaged over the entire catchment for the present climate is 1,840 mm y¹. There are several reservoirs in the catchment, which makes the analysis of the impact of climate change on hydropower production interesting. Moreover, this region is climatologically prone to floods that are characterised by higher specific discharges because of the southern climatological regime, which is influenced by the Mediterranean cyclogeneses, and is thus of particular interest with respect to future climate response.

Kl. Emme catchment. The catchment is located in central Switzerland (46.9° N, 8° E). It has a total drained area of 477 km² and an elevation range between 600 and 2,275 m with a mean of 1,172 m. The precipitation average over the entire catchment for the present climate is 1,800 mm y⁻¹. The catchment is glacier free and mostly covered by natural vegetation, except for small cropland areas and villages. The river flow regime is close to natural conditions without any major withdrawals for irrigation or hydropower uses.

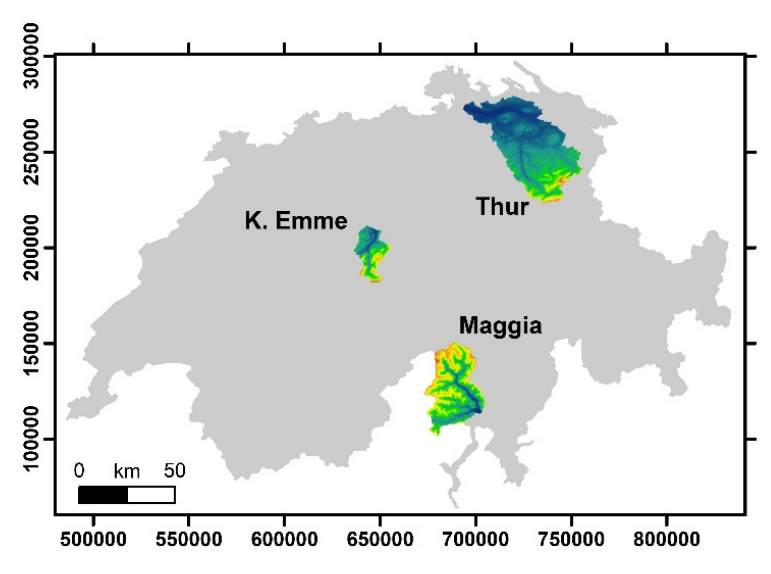


Figure 2 – Location map of the catchments. Coordinates are in Swiss projection (CH-1903) in m.

4 DATA

Present climate. Climate data (precipitation, temperature, and radiation) were obtained from the Swiss Federal Office for Meteorology and Climatology (MeteoSwiss) from three different sources: ground stations (summarized in Table 1), weather radar system (Gabella et al., 2005; Germann et al., 2006) and grid-data products (RhiresD - Schwarb, 2000 and TabsY - Frei, 2014). Cloud cover data and wind speed at 500 hPa level were obtained from the MERRA-2 reanalysis product (Gelaro et al., 2017) and aerosols optical depth were calculated based on data derived from the AERONET network (Holben et al., 1998).

Future climate. Nine regional climate models were chosen from the CH2018 archive to be used in this project (Table 2). The climate models are part of the EURO-CORDEX initiative (Jacob et al., 2014). The original simulations were performed at a spatial resolution of 12.5 km \times 12.5 km. The climate model outputs were processed within the CH2018 project, quantile mapped and regridded for the Switzerland domain at 2 km \times 2 km resolution.

Streamflow data. Hourly and daily streamflow estimates for gauged locations within the three catchments were obtained from BAFU archives (Table 3).

Table 1 – List of ground stations from MeteoSwiss.

Catchment	Station name
	Cimetta
	Acquarossa / Comprovasco
	Piotta
Maggia	Robiei
Maggia	Ulrichen
	Cavergno Bignasco
	Camedo
	Osservatorio Ticinese Locarno
	Ebnat-Kappel
	Güttingen
	Oberriet
Thur	Säntis
	Schaffhausen
	St. Gallen
	Aadorf / Tänikon
	Vaduz
	Wädenswil
Kl. Emme	Luzern
	Napf
	Pilatus

Table 2 – List of climate models from the CH2018 archive that were used in this project.

ID	RCM	Driving GCM
1	CLMcom-CCLM4-8-17	ICHEC-EC-EARTH
2	DMI-HIRHAM5	ICHEC-EC-EARTH
3	SMHI-RCA4	ICHEC-EC-EARTH
4	CLMcom-CCLM4-8-17	MOHC-HadGEM2-ES
5	SMHI-RCA4	MOHC-HadGEM2-ES
6	SMHI-RCA4	IPSL-IPSL-CM5A-MR
7	CLMcom-CCLM4-8-17	MPI-M-MPI-ESM-LR
8	MPI-CSC-REMO2009	MPI-M-MPI-ESM-LR
9	SMHI-RCA4	MPI-M-MPI-ESM-LR

Table 3 – List of streamflow recording stations that were used in this project.

Catchment Station name		BAFU code
	Maggia - Locarno, Solduno (Outlet)	2368
Maggia	Maggia - Bignasco, Ponte nuovo	2475
	Riale di Calneggia - Cavergno, Pontit	2356
	Thur-Andelfingen (Outlet)	2044
	Thur-Halden	2181
	Thur-Jonschwil	2303
Thur	Glatt-Herisau, Zellersmühle	2305
THUI	Murg-Frauenfeld	2386
	Murg-Wängi	2126
	Rietholzbach-Mosnang, Rietholz	2414
	Necker-Mogelsberg, Aachsäge	2374
V1 F	Kl. Emme-Emmen (Outlet)	2634
Kl. Emme	Kl. Emme-Werthenstein, Chappelboden	2487

5 RESULTS

Results of the validation of the weather generator model and the hydrological model are presented first, followed by the results of the changes in climate and hydrology.

5.1 VALIDATION OF AWE-GEN-2D

The AWE-GEN-2d model was validated for reproducing the climate variables needed for the hydrological simulations (e.g. precipitation, near-surface air temperature, cloud cover, and radiation) in the three catchments, following the same validation procedure introduced by Peleg et al. (2017, 2020). In this report, only the key validation aspects are presented. Figure 3 presents a comparison between the observed and simulated mean annual temperature of the three

catchments. Most grid cells in the Kl. Emme show a difference between observed and simulated temperatures that are smaller than 1°C. The same holds for the Thur catchment, where most grid cells show an overestimation of the simulated temperature by up to 1 °C, except for the high mountainous region in the south-east where the model produces an underestimation of the temperature by up to 3°C. The differences between observed and simulated temperature in the Maggia catchment are much higher than in the other two catchments, reaching up to ±6 °C difference. However, it seems that there is a shift of 2-4 km along the east-west axis in the location of the valley and mountains between the observed and simulated maps that may be the source of this apparent error.

Figure 4 compares the annually averaged precipitation maps. Precipitation is well captured in the Kl. Emme catchment. The comparison may suggest an overestimation of model outputs over the catchment, but the maximum deviation is in the order of 4%, which compares well with the expected natural variability of precipitation for this region (Fatichi et al., 2016a; Peleg et al., 2017). In the Thur catchment, the model underestimates precipitation in the north of the catchment (low elevation region) and overestimates precipitation in the southern (mountainous) part of the catchment. Yet, the under/overestimation is also in this case very small, in the order of 3%. In the Maggia catchment, the model generally overestimates precipitation (up to 9%), except for a single grid cell where underestimation is recorded (of 8%). We note that the area in the south-west of the catchment lies outside of Switzerland border, thus precipitation is estimated using other product then RhiresD.

Temperature and precipitation were also validated at sub-daily (hourly) and seasonal scales. This was done using observed data from climate stations that are located within or near the borders of the catchments. Here, we present the validation using a single climate station for each of the catchments. The observed and simulated diurnal cycle of temperature is presented in Figure 5. For all locations, the timing of the maximum and minimum daily temperatures and the diurnal dynamics are well simulated. The largest offset in hourly temperature in the K1. Emme is less than 0.5 °C. The largest difference between observed and simulated hourly temperature in the Thur catchment is in the order of 1.3 °C, which is still within an acceptable range. In the Maggia catchment, the model overestimates the hourly maximum peak temperature and underestimates the minimum daily hourly temperature by up to 2 °C.

The model captures the seasonal dynamics of temperature well for all three catchments (Figure 6). The model overestimates summer temperatures in the Thur catchment (up to 2 °C) and in the Maggia catchment (up to 0.5 °C). We note that differences in temperature in the order of few °C are acceptable as they are within the error in monthly temperature estimation that depends on the sample size (i.e. the number of years/months).

The model's abilities to reproduce the seasonal dynamics were also explored for precipitation (Figure 7). The monthly mean precipitation and the natural variability in precipitation (presented using the 5-95th percentile range) are simulated well in the Kl. Emme and Maggia catchments but overestimated for the winter period (by up to 35 mm) on Thur.

Finally, Figure 8 illustrates the model abilities to reproduce extreme precipitation at the hourly scale. The model was not calibrated to simulate extreme precipitation at sub-daily scales explicitly (calibration was done on daily estimates). Yet, a good fit is achieved between the observed

and simulated extremes for most locations, especially between the 1 and 30 years return periods (for which records are available). In the Kl. Emme a small overestimation of the extreme precipitation intensity is detected at some of the locations where observations are available, while a small underestimation is found for several locations in the Thur catchment. We note, however, that the uncertainty in the observed gridded estimates obtained from MeteoSwiss is high (Scherrer et al., 2016).

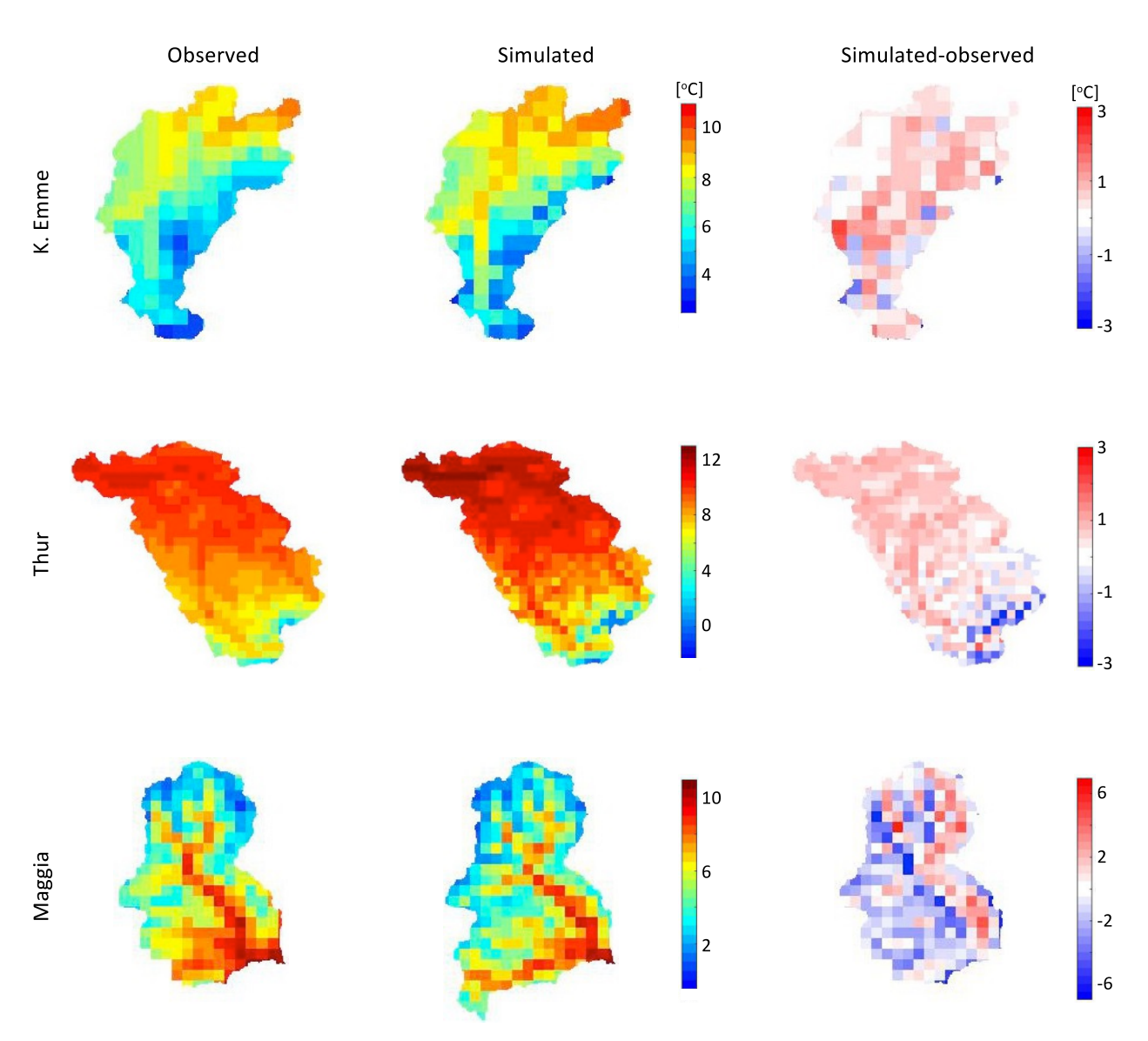


Figure 3 – Mean near-surface air temperature for the period 1982-2015 as obtained from the TabsY product (observed) in comparison with the mean ensemble generated by AWE-GEN-2d (simulated).

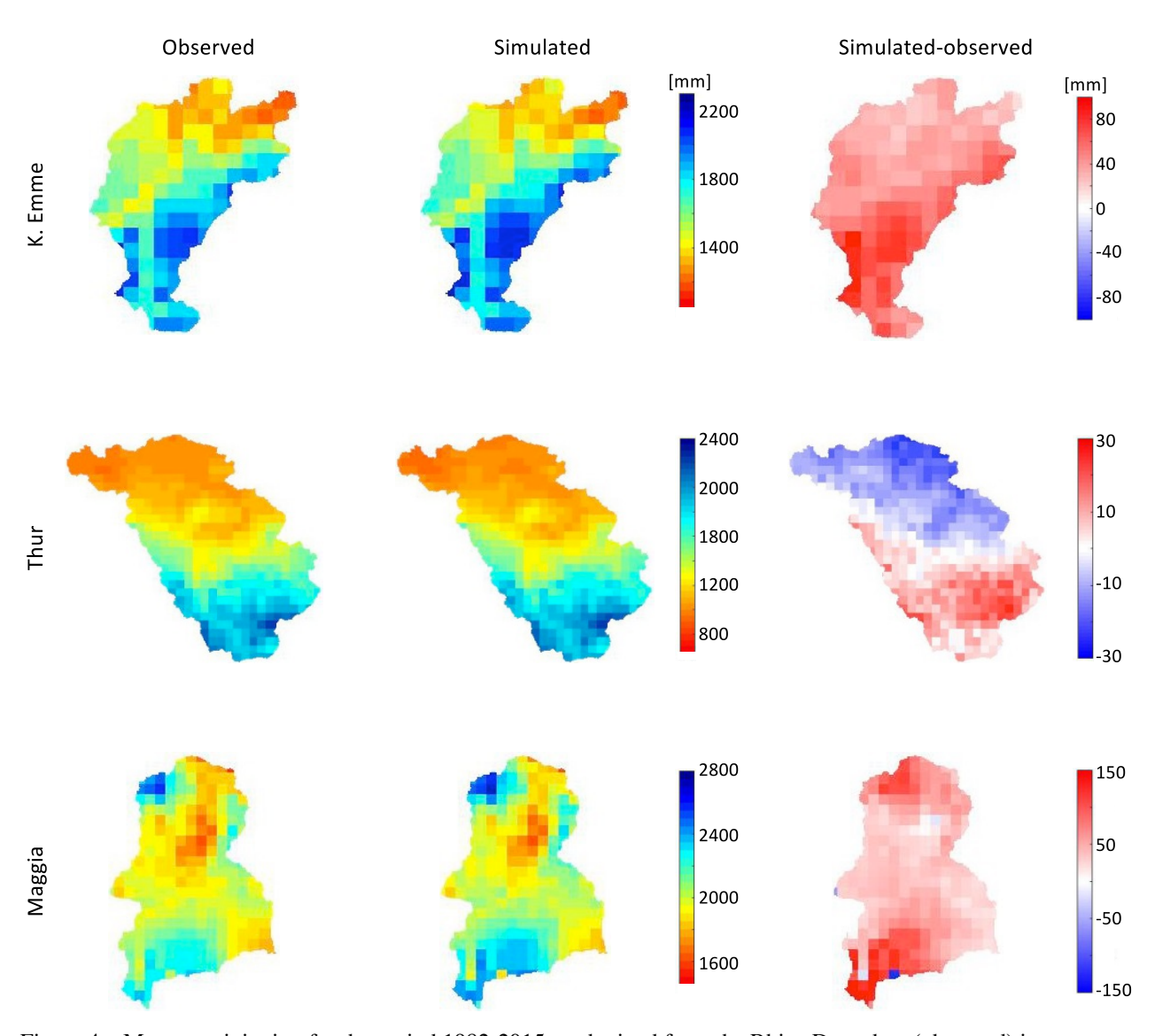


Figure 4 – Mean precipitation for the period 1982-2015 as obtained from the RhiresD product (observed) in comparison with the mean ensemble generated by AWE-GEN-2d (simulated).

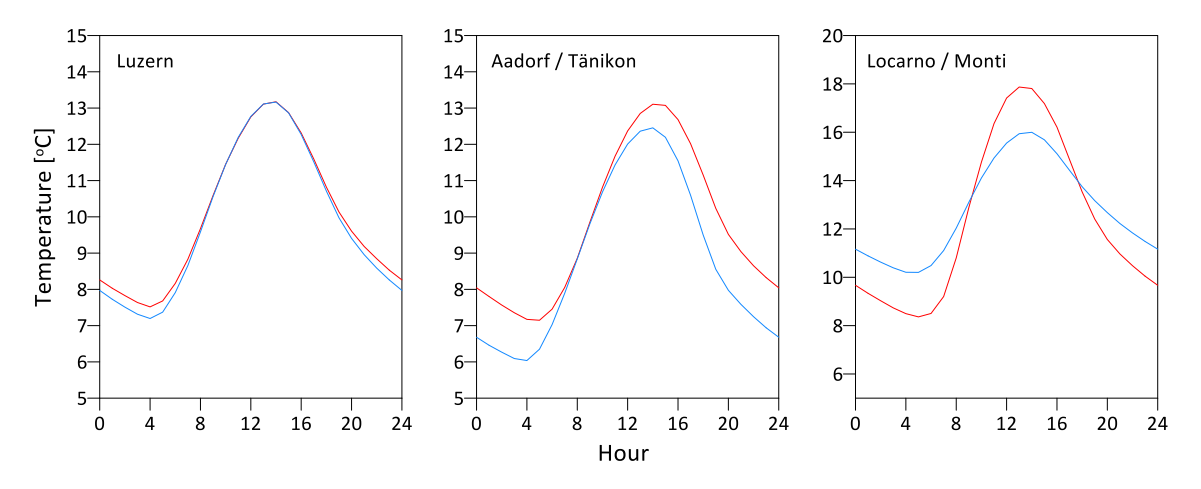


Figure 5 – Observed mean diurnal cycle of temperature (blue) and simulated (red) computed from the generated climate ensemble. Location: Luzern – Kl. Emme, Aadorf – Thur, and Locarno – Maggia.

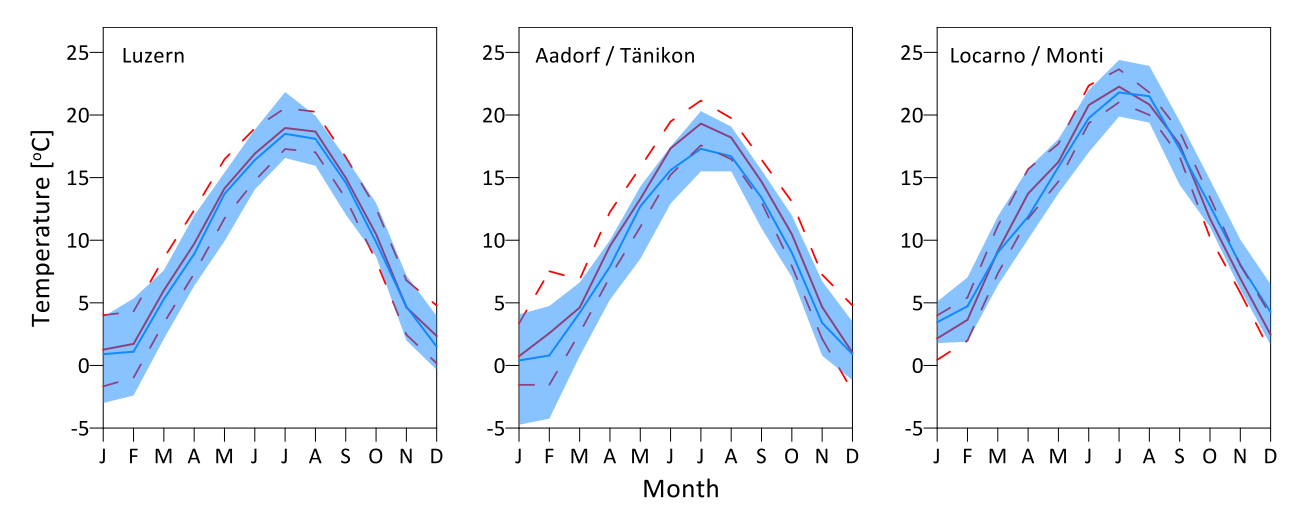


Figure 6 – A comparison between observed and simulated temperatures for each month. The blue and red solid lines represent the observed and simulated median values (respectively) and the bounded areas represent the observed (blue area) and simulated (dashed lines) 5–95th percentile range (respectively). The observed period covers 34 years of data (1982–2015), while simulations represent the mean of 30 realizations of 30 years each.

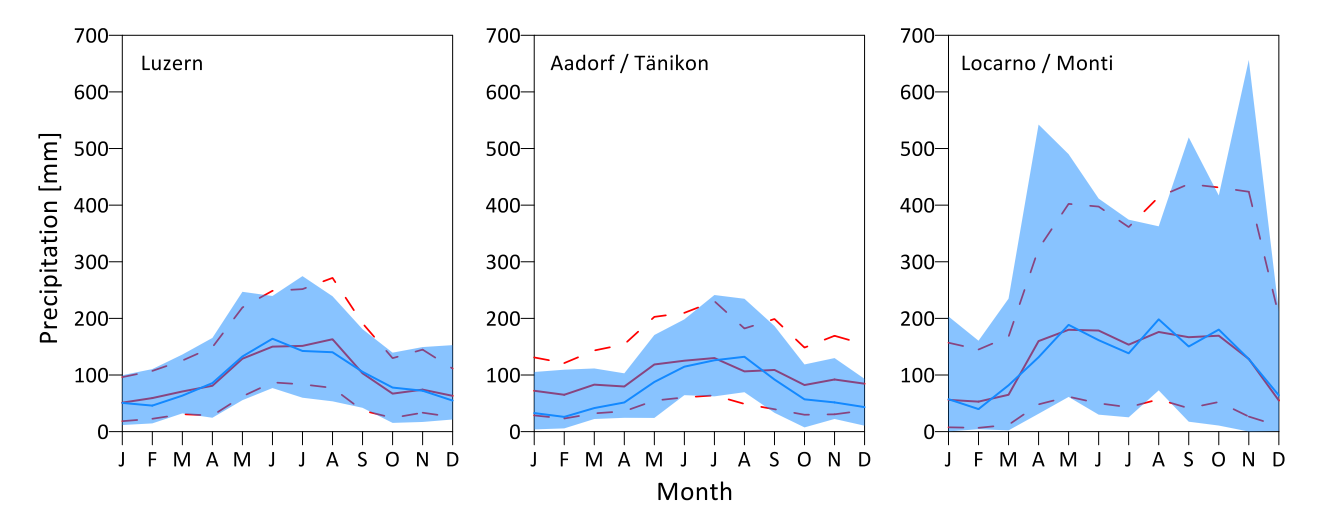


Figure 7 – A comparison between observed and simulated precipitation for each month. The blue and red solid lines represent the observed and simulated median values (respectively) and the bounded areas represent the observed (blue area) and simulated (dashed lines) 5–95th percentile range (respectively). The observed period covers 34 years of data (1982–2015), while simulations represent the mean of 30 realizations of 30 years each.

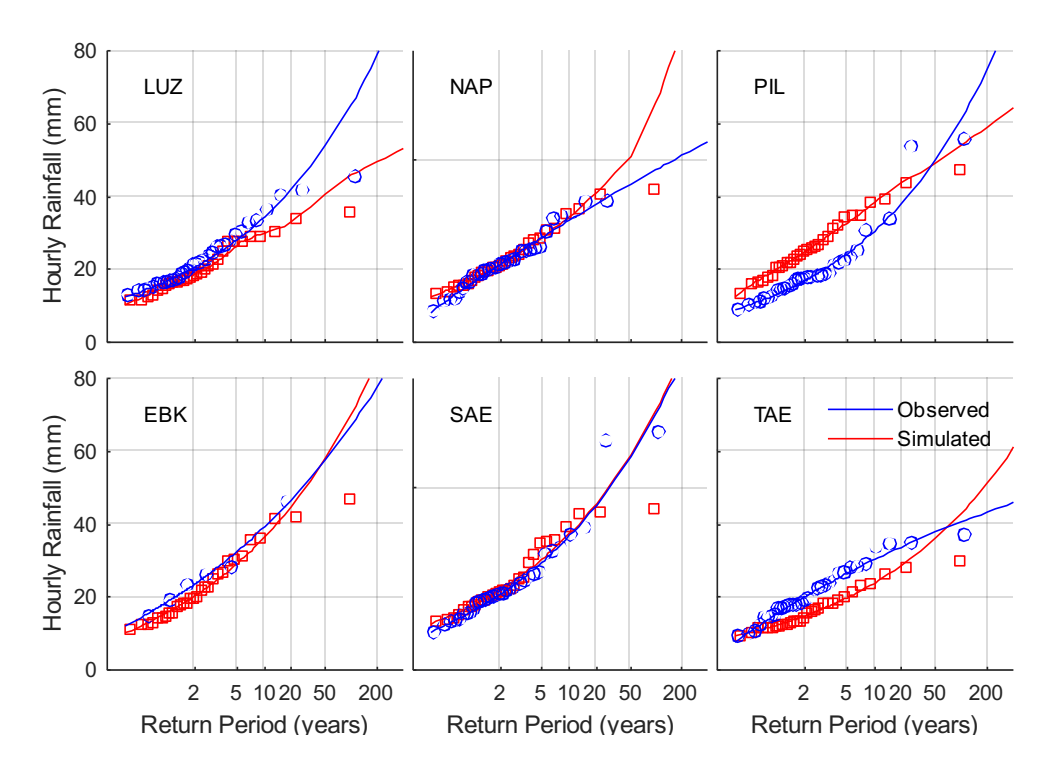


Figure 8 – Validation of annual maximum precipitation intensity at the hourly scale for different return periods in the Kl. Emme (top row) and Thur (bottom row) weather stations. The solid lines represent the observed (blue) and simulated (red) precipitation intensity computed by fitting GEV distribution to the data. The observed period covers 34 years of data (1982–2015), while simulations represent the mean of 30 realizations of 30 years each.

5.2 Validation of Topkapi-ETH

The KI. Emme and Thur catchments are considered as natural catchments, i.e. their streamflow is not altered by regulated by infrastructures and/or human activities, so that the model performance at the outlet of the catchment could be evaluated against observed data. The Maggia catchment is completely regulated due to the hydropower operation, and thus the model was evaluated against the flow into the hydropower reservoirs instead, which are considered as a natural flow (Figure 9).

Topkapi-ETH was validated at the hourly and monthly scales on available streamflow observations. First, a Nash–Sutcliffe Efficiency index (NSE) was computed for the period between 2000 and 2009 at the hourly scale, yielding values of 0.74 for the Kl. Emme catchment and 0.57 for the Thur catchment. An example of Topkapi-ETH simulation is presented in Figure 10.

At the monthly scale (Figure 11), the model preserves the high NSE values (0.76 and 0.78 for the Kl. Emme and Thur catchments, respectively), but underestimates mean monthly flows for most of the months in the Kl. Emme catchment (up to 30%) and for October-November months in the Thur catchment (up to 20%). However, the model correctly reproduces the seasonal dynamics and the natural variability of streamflow. Examining longer periods (i.e. extending the comparison beyond the years used for the calibration of the model), confirms the monthly NSE values of 0.74 for the Kl. Emme (1986-2009) and 0.76 for the Thur (1982-2009) catchments.

In addition to the NSE score, the model simulations were evaluated against the maximum annual streamflow observed at the outlets of the Kl. Emme and Thur catchments (Figure 12). The model captures the hourly streamflow extremes for the return periods between 1 and 30 years well but underestimates the low-frequency streamflow extremes in Thur while overestimating the low-frequency streamflow extremes (i.e. above the 100-year return period) in the Kl. Emme. As for the precipitation extremes, the observed data is characterized by high uncertainties (Hilker et al., 2009), which are of the same order of magnitude of the confidence intervals presented in Figure 12.

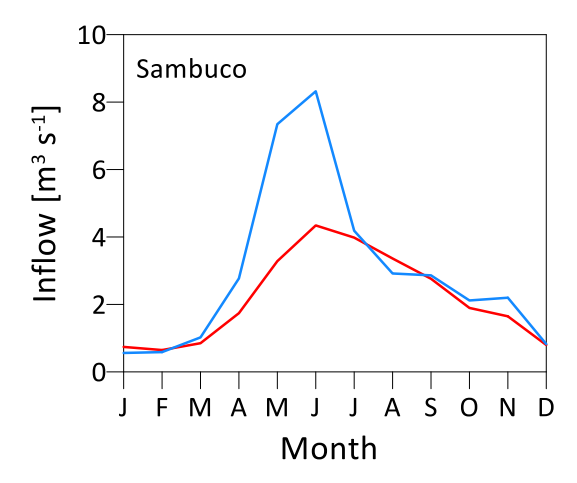


Figure 9 – A comparison between observed and simulated inflow for each month (2006-2015, excluding 2010) in Sambuco reservoir. The blue and red lines represent the observed and simulated mean values (respectively).

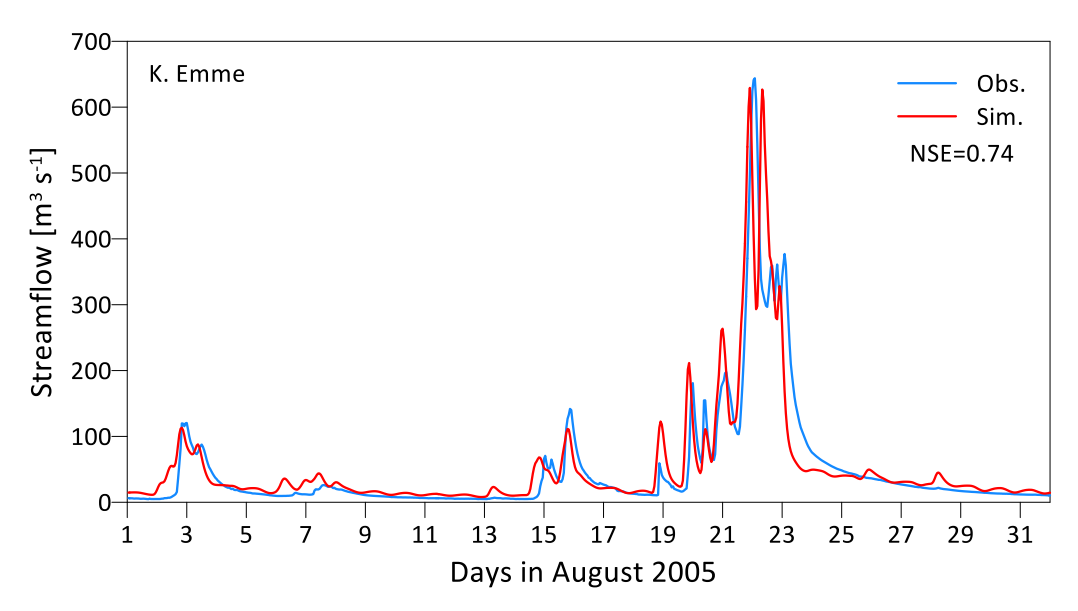


Figure 10 – A comparison between observed (blue) and Topkapi-ETH simulated (red) streamflow (outlet of Kl. Emme catchment). NSE refers to the Nash–Sutcliffe efficiency that was computed at the hourly scale for the period 2000-2009.

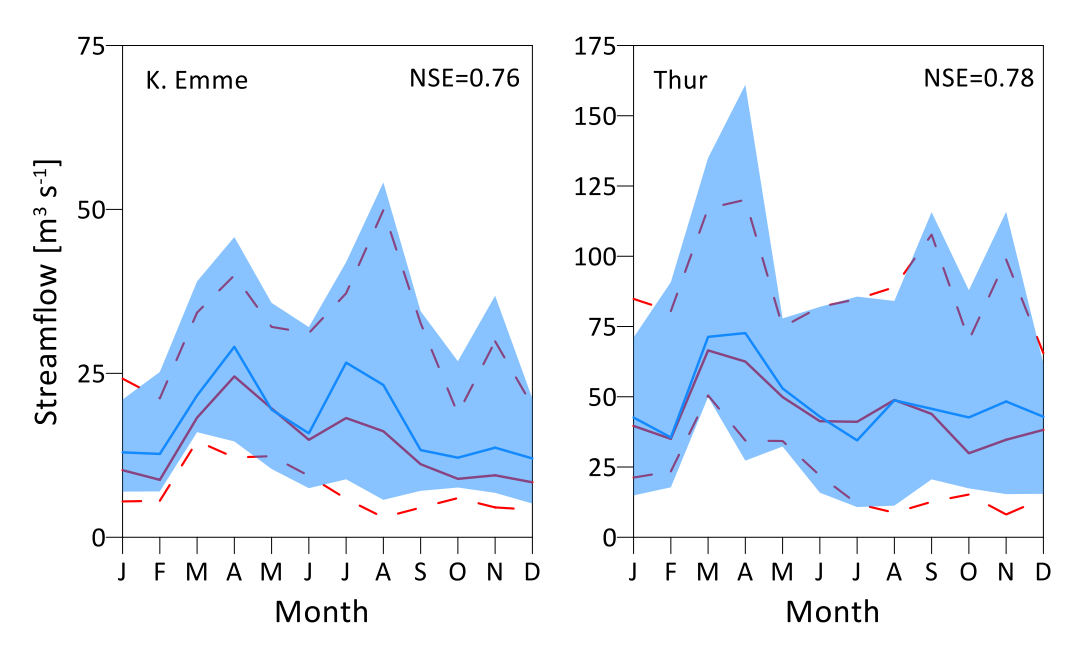


Figure 11 – A comparison between observed and simulated streamflow for each month (2000-2009). The blue and red solid lines represent the observed and simulated median values (respectively) and the bounded areas represent the observed (blue area) and simulated (dashed lines) 5–95th percentile range (respectively).

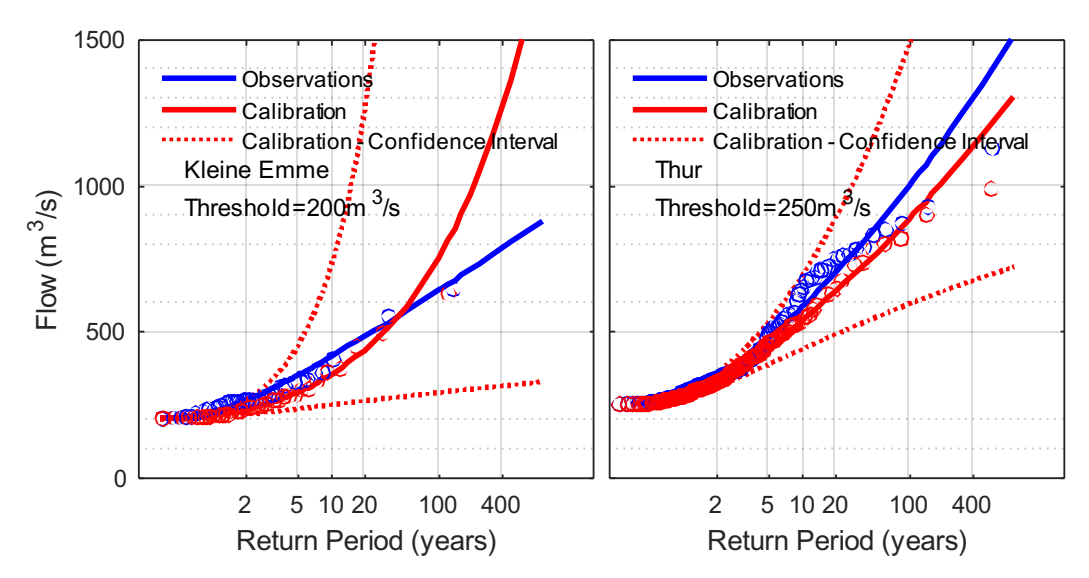


Figure 12 – Comparison between observed and simulated peak-over-threshold at the hourly scale for different return periods in the Kl. Emme (left) Thur (right) catchments. The solid lines represent the observed (blue) and simulated (red) streamflow computed by fitting a Generalized Pareto distribution to the recorded data for the 2000–2009 period. The plotting positions were calculated using Gringorten's equation and the return periods are calculated via the reduced variate method.

5.3 CHANGES IN CLIMATE

The changes in climate, downscaled using the weather generator, are presented here first at the domain scale (i.e. as climate variables averaged over the catchments) and, after, are analysed with respect to their heterogeneities within the catchments, focusing on spatial variability of the changed simulated at the $2 \text{ km} \times 2 \text{ km}$ scale.

5.3.1 Domain scale

The results are discussed for three periods: 2020-2049 ('early mid-century' from thereafter), 2040-2069 ('mid-century') and 2070-2099 ('end of the century'). The reference for the 'present' climate is the simulation of the climate as observed between 1976 and 2005.

As expected, all downscaled climate trajectories indicate an increase in temperature over the catchments that accelerate when approaching the end of the century (Figure 13). The uncertainty in the increase of temperature is quite significant for each period (expressed as the minimum-maximum range of the multi-model mean) and is mainly composed of the climate model uncertainty (Hingray and Saïd, 2014). For the K1. Emme catchment, the multi-model mean indicates an increase of temperature in the range of 0.4-2°C, 1.4-3°C and 3-5.3°C, respectively, for the three periods indicated above. A similar increase in temperature is projected for the Thur catchment (0.4-2°C, 1.4-3°C and 2.7-5.2°C), while higher temperatures are predicted in the Maggia catchment (0.9-2°C, 1.7-3.3°C and 3.4-6°C).

The changes in precipitation are less homogenous (Figure 14). In the K1. Emme catchment, 8 out of 9 downscaled climate trajectories point on a decrease in precipitation already in the early midcentury period. For the mid-century period, 7 out of 9 downscaled climate trajectories indicate on reduction in precipitation and at the end of the century, only 6 out of the 9 trajectories agree on a negative trend in precipitation. As a result, the uncertainty around the multi-model mean increases considerably toward the end of the century: from a range of -12-(+2%) for the early midcentury to -18-(+7%) for the mid-century and finally to -16-(+8%). Conversely, all climate models agree on an increasing trend in precipitation for the Thur catchment, in a range that varies between 6-33%, 9-34% and 14-40% respectively for the three considered periods. In the Maggia catchment, there is a general agreement between the downscaled climate trajectories of a decrease in precipitation amounts for the early mid-century period. However, while some of the downscaled trajectories indicate a continuous decreasing trend for precipitation toward the end of the century, others point to a recovery in precipitation amounts. The range of uncertainty around the multi-model is thus relatively stable in time in the range of -18% to +5%.

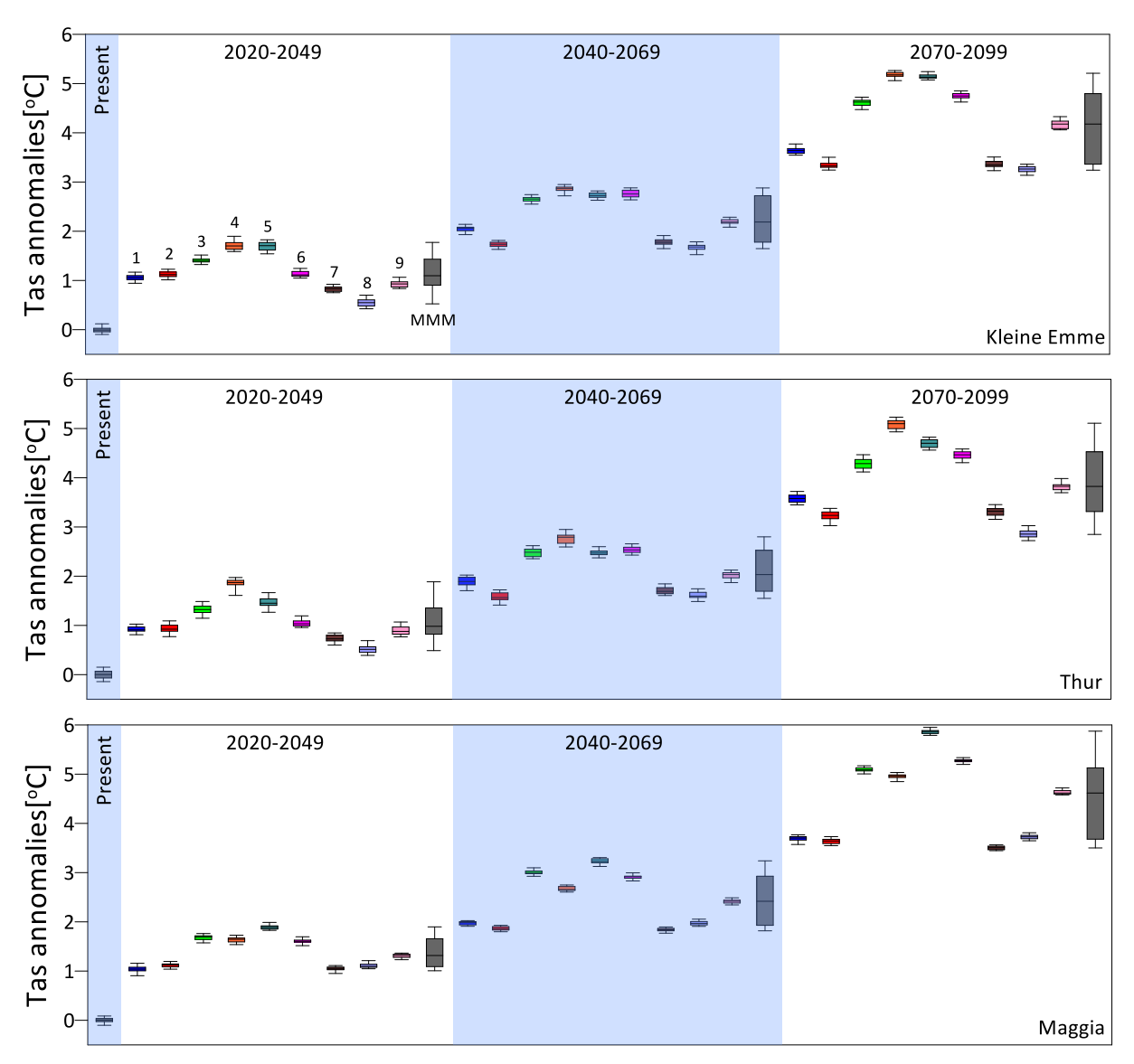


Figure 13 – Differences in mean annual temperature between the present period (1976-2005) and future periods for the Kl. Emme, Thur and Maggia catchments. Numbers 1 to 9 refer to the different climate models (see Table 1) and MMM refers to the multi-model mean. Box plots for the present and 1 to 9 simulations represent the stochastic uncertainty for each climate trajectory, and MMM represents the combination of stochastic and climate model uncertainty. Central lines in the box plots represent the median of the mean annual temperature of the ensemble, while the boxes and whisker lines represent the 25-75th and 5-95th percentile range of the data. The simulated ensemble for each climate trajectory is composed of 30 realizations of 30 years each, bootstrapped from an archive of 100 years.

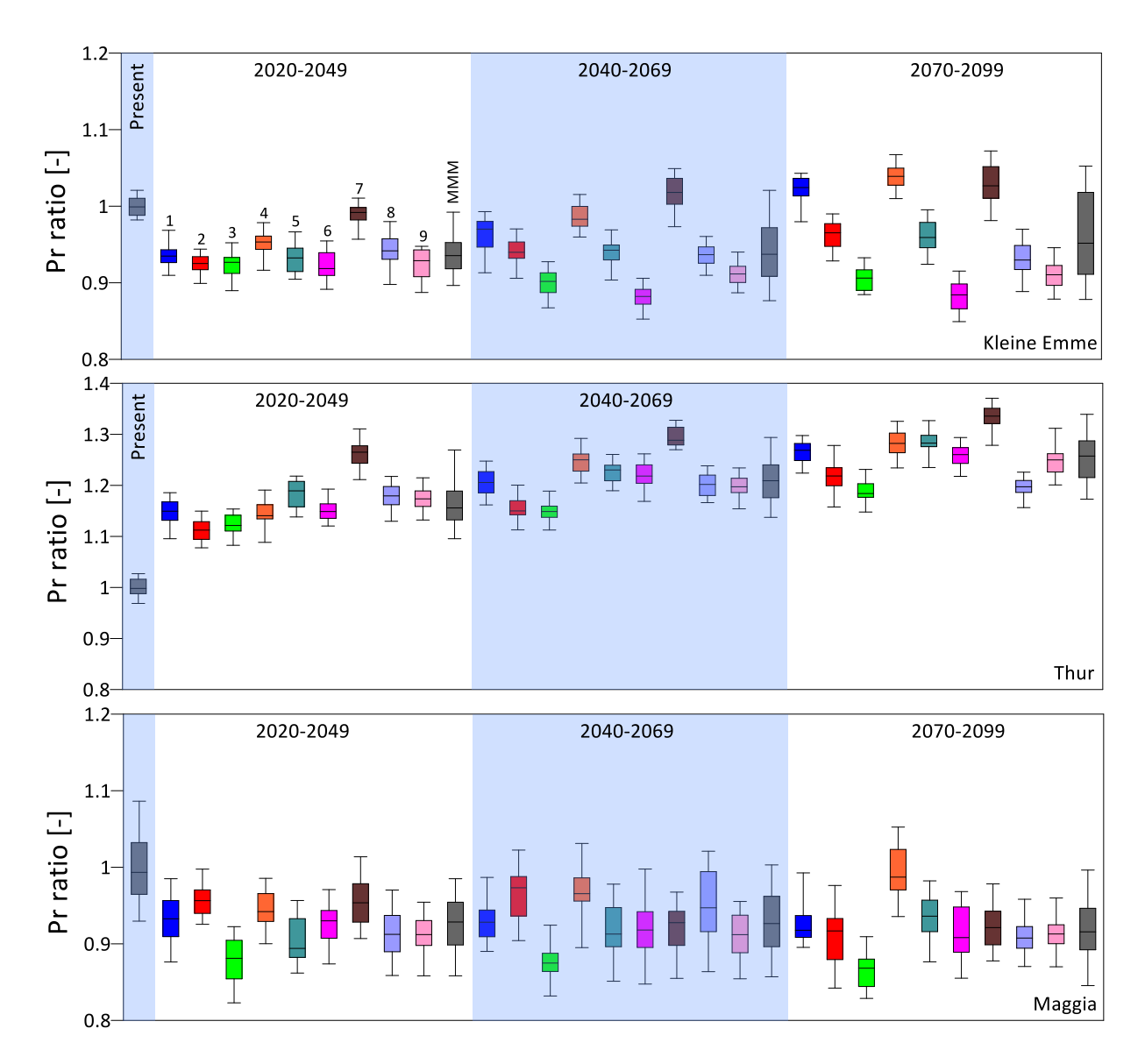


Figure 14 – Similar plot as Fig. 13, but for the ratios of mean annual precipitation.

The changes in precipitation extremes were examined at the hourly (Figure 15) and daily (Figure 16) scales. The direction of change is not completely clear in the Kl. Emme and Thur catchments. In the Kl. Emme, for the 2-year return period, the multi-model mean practically points on no change in precipitation extreme as some model force an increase while others suggest decreasing to the precipitation intensity. In Thur, most downscaled models projected an increase in extreme precipitation intensity, but the two models (6 and 9) that indicate 'no change' force the multi-model mean to converge to the present climate mean value. The stochastic uncertainty range for each of the individual downscaled climate trajectories (1 to 9) increases with increasing return periods. As discussed by Peleg et al., 2019 this is expected and in agreement with the stochastic uncertainty range of the extreme precipitation simulated for the present climate. As a result, the uncertainty range of the multi-model mean largely overlaps with the stochastic uncertainty of present climate, thus suggesting that no statistically significant change in extreme precipitation intensity can be detected for return periods of 5-year and higher. As opposed to Kl.

Emme and Thur catchments, a clear reduction in extreme precipitation intensity in the order of 20% (hourly) to 40% (daily) is detected in the Maggia catchment. Unexpectedly, the stochastic uncertainty for future climate simulations is not increasing with higher return periods. As an increase in the stochastic uncertainty is seen for the simulations of the present climate, we conclude that the climate models forced the weather generator to unrealistic values. Therefore, any hydro-climatic conclusion related to extremes and their uncertainty should be considered with caution in the Maggia basin.

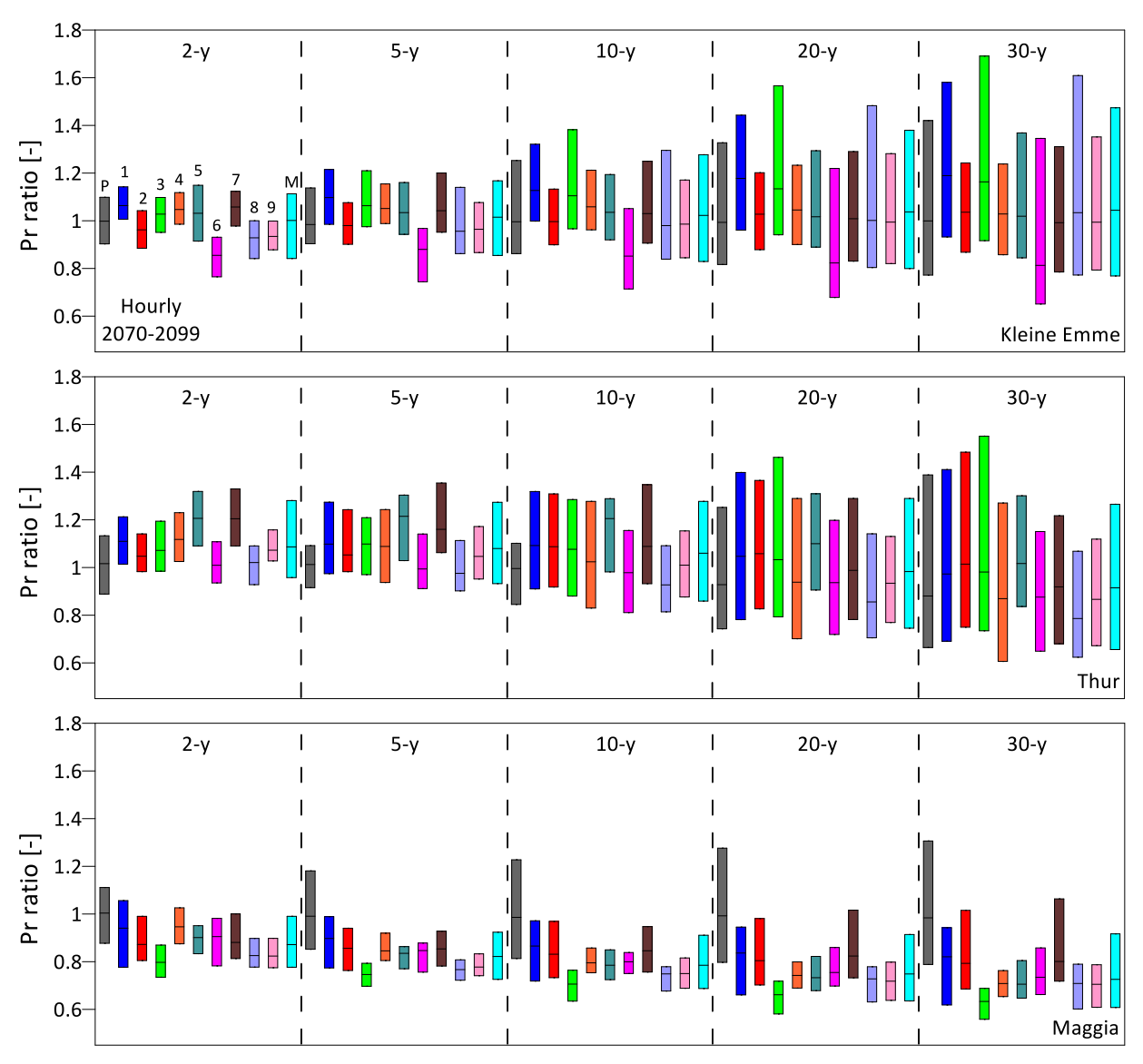


Figure 15 – The ratio between annual maximum precipitation for a given return period of present climate (1976-2005) and end of the century climate (2070-2099) at the hourly scale. Numbers 1 to 9 refer to the different climate models (see Table 1) and M refers to the multi-model mean. Box plots for the present and 1 to 9 represent the stochastic uncertainty for each climate trajectory, and M represents the combination of stochastic and climate model uncertainty. Central lines in the box plots represent the median of mean annual maximum precipitation intensity computed from the simulated ensemble using GEV distribution, while the boxes represent the 5-95th percentile range of the data. The simulated ensemble for each climate trajectory is composed of 30 realizations of 30 years each, bootstrapped from an archive of 100 years.

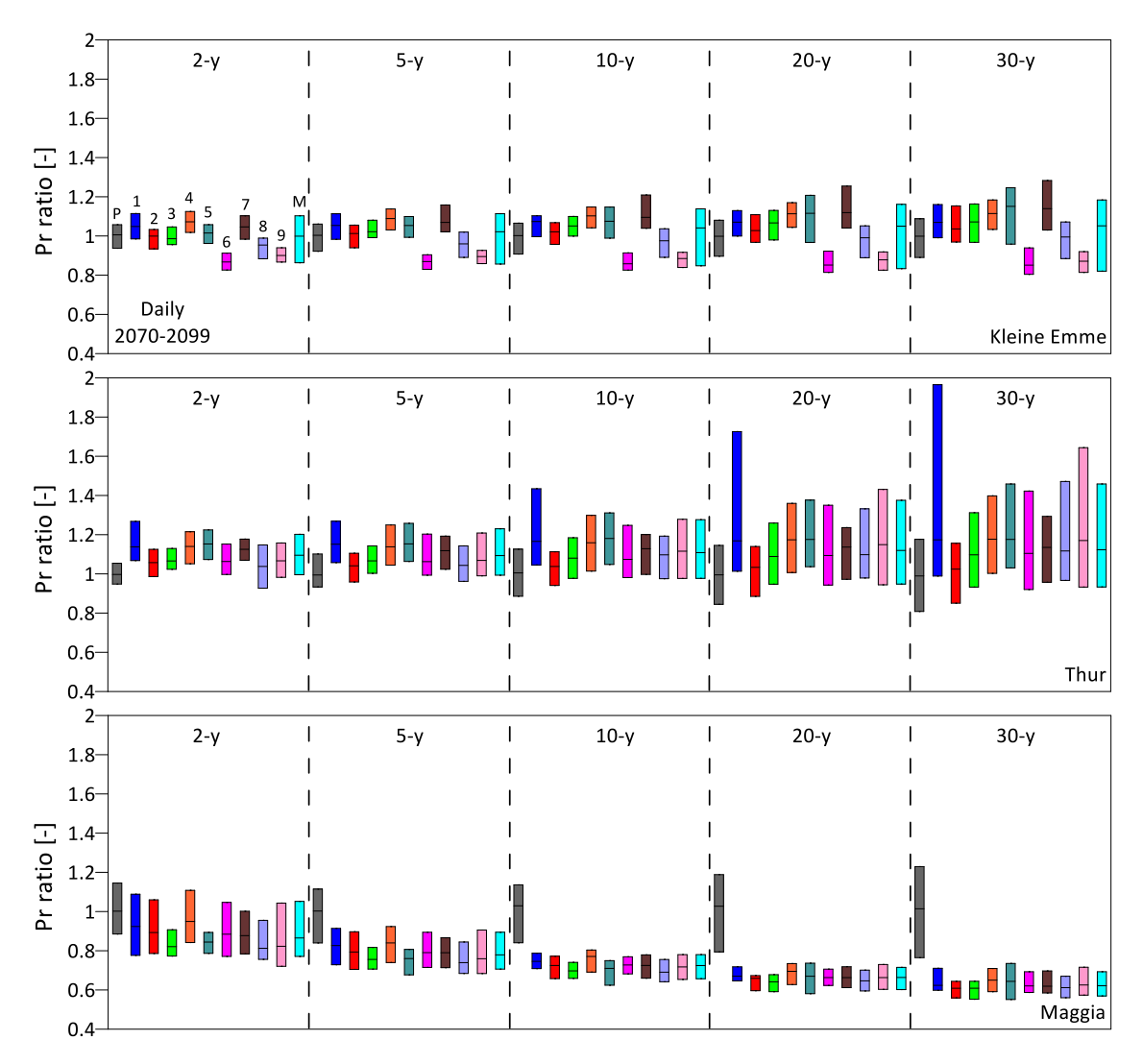


Figure 16 – Similar plot as Fig. 15, but on a daily scale.

5.3.2 The 2-km scale

The spatial changes in climate variables within the catchments were also explored (Figure 17 and Figure 18). There is a higher increase in temperature during summer months in both K1. Emme and Thur catchments (Figure 17) in comparison to the other seasons. The temperature changes are not following the topography, and in fact, the change seems to be the same over the entire domain with a small stochastic variability in space, which can be regarded as to a "white noise". This can be a result of using RCMs characterised by a resolution of $12.5 \text{ km} \times 12.5 \text{ km}$, which do not resolve topography sufficiently to capture properly possible changes in mountainous regions.

Precipitation is projected to decrease during summertime but increase during wintertime (Figure 17) in all catchments. On the contrary to temperature, precipitation exhibit a spatially variable pattern of change. In the Kl. Emme and Thur catchments, precipitation tends to decrease over the mountainous regions (southern areas of the catchments) and tends to increase in the relatively low areas toward the outlets of the catchments. Conversely, in the Maggia catchment,

precipitation is generally decreasing, with a higher magnitude of decrease over the mountainous areas in comparison to the lower elevated regions.

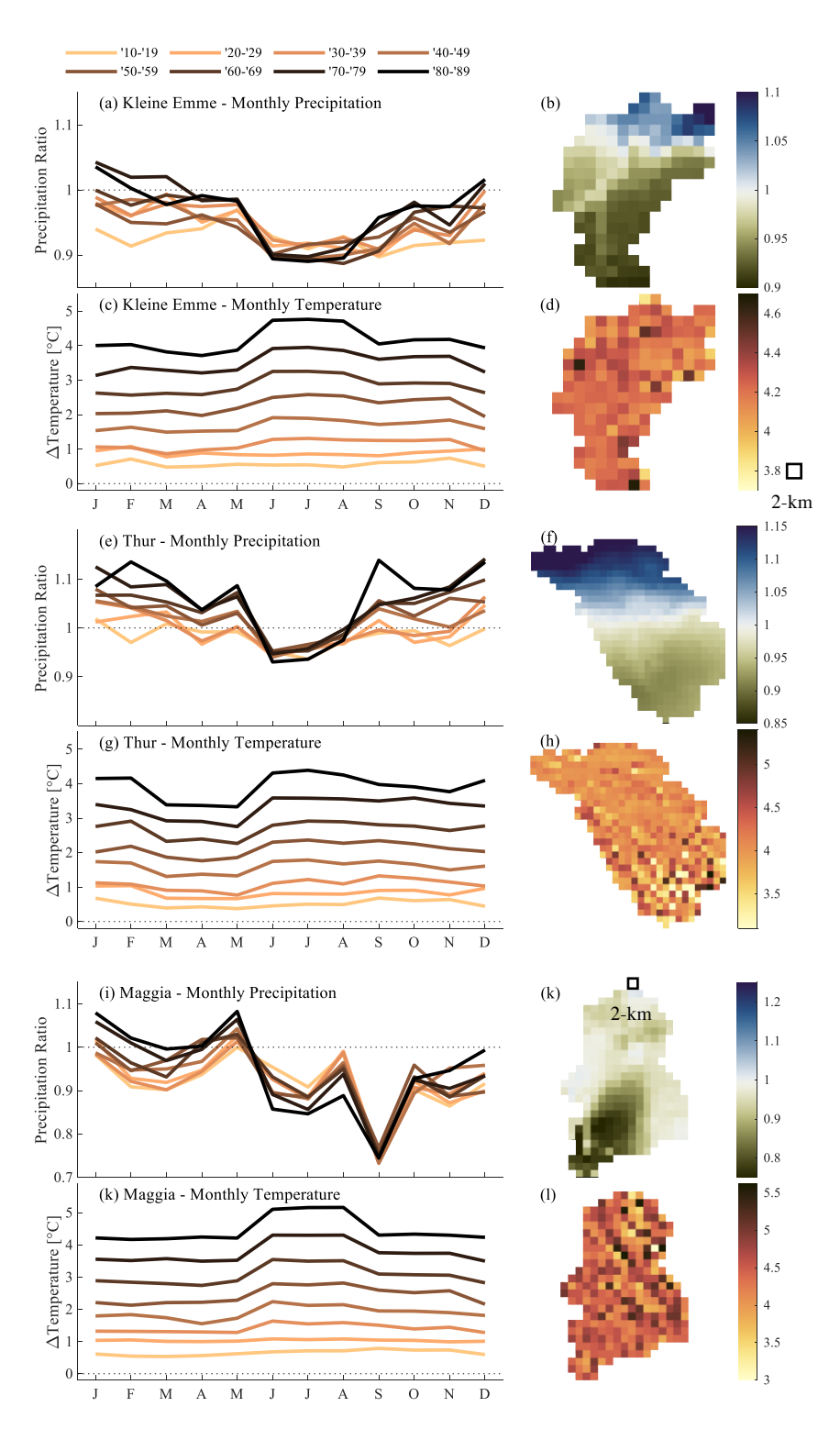


Figure 17 – Projected multi-model mean anomalies in climate variables relative to the present climate (1976–2005) in the Kl. Emme (a–d), Thur (e–h) and Maggia (i-l). Panels (a, e), (c, g) and (i, k) show the monthly precipitation and temperature anomalies for each future period, respectively, whereas panels (b, f), (d, h) and (j, l) show the spatial distribution of the annual anomaly by the end of the century (2080–2089).

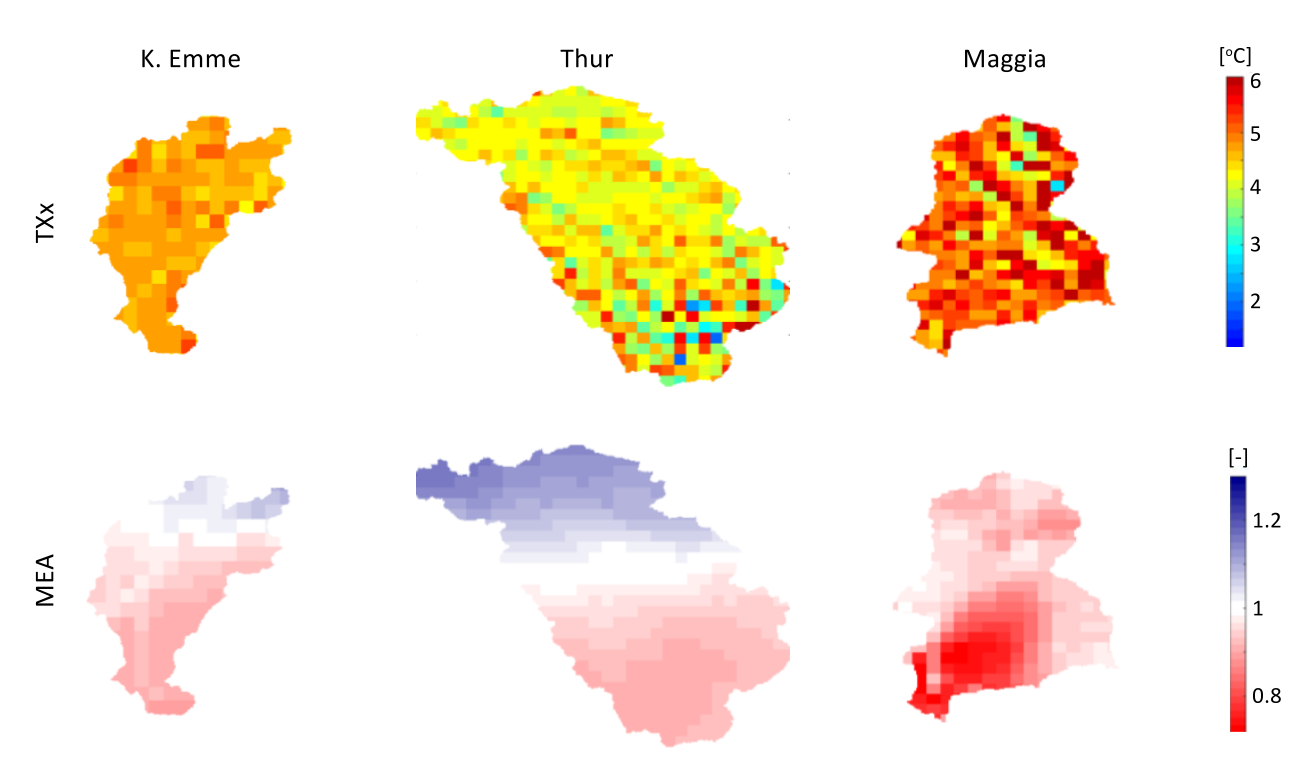


Figure 18 – Differences in the temperature of the hottest day in the year (annual maximum of daily T_{max} , TXx) and ration change of mean daily rainfall (MEA) between the present climate (1976-2005) and end of the century scenarios (2070-2099, multi-model mean).

5.4 CHANGES IN HYDROLOGY

5.4.1 Changes of the mean streamflow regime at the catchment outlets (KI. Emme and Thur)

Analysing the changes in annual streamflow at the outlets of the Kl. Emme and Thur catchments, a clear decrease in flow volumes is seen already for the early-mid-century period (Figure 19). The downscaled scenarios driven by the multi-model-mean indicate a reduction in the order of 10% for both catchments, with an uncertainty range of -19% to +2% for the Kl. Emme catchment and -23% to +8% for the Thur catchment. In fact, in both catchments, the trajectories of scenarios driven by one single model (model 7) lead to unchanged conditions in comparison to the present. For the mid-century and end of the century periods, the predictions of the changes in streamflow become highly uncertain. This is because several climate model show more variable predictions, showing, for instance, an increase in the mean annual streamflow in comparison to the present in later periods (for example, model 4), thus leading to downscaled climate trajectories ultimately generating highly uncertain streamflow predictions. As a result, the uncertainty around the multi-model mean increases with time, yet the mean value itself remains rather stable until the end of the century (at around -10% change).

The analysis of seasonal changes in streamflow (Figure 20) points at both catchments experiencing an increase in winter flows by up to 40%. On the contrary, summer flows are predicted to decrease by 20% in the Kl. Emme and 40% in the Thur. The magnitudes and uncertainties in the decrease of summer flows and increase of winter flows are increasing toward the end of the century.

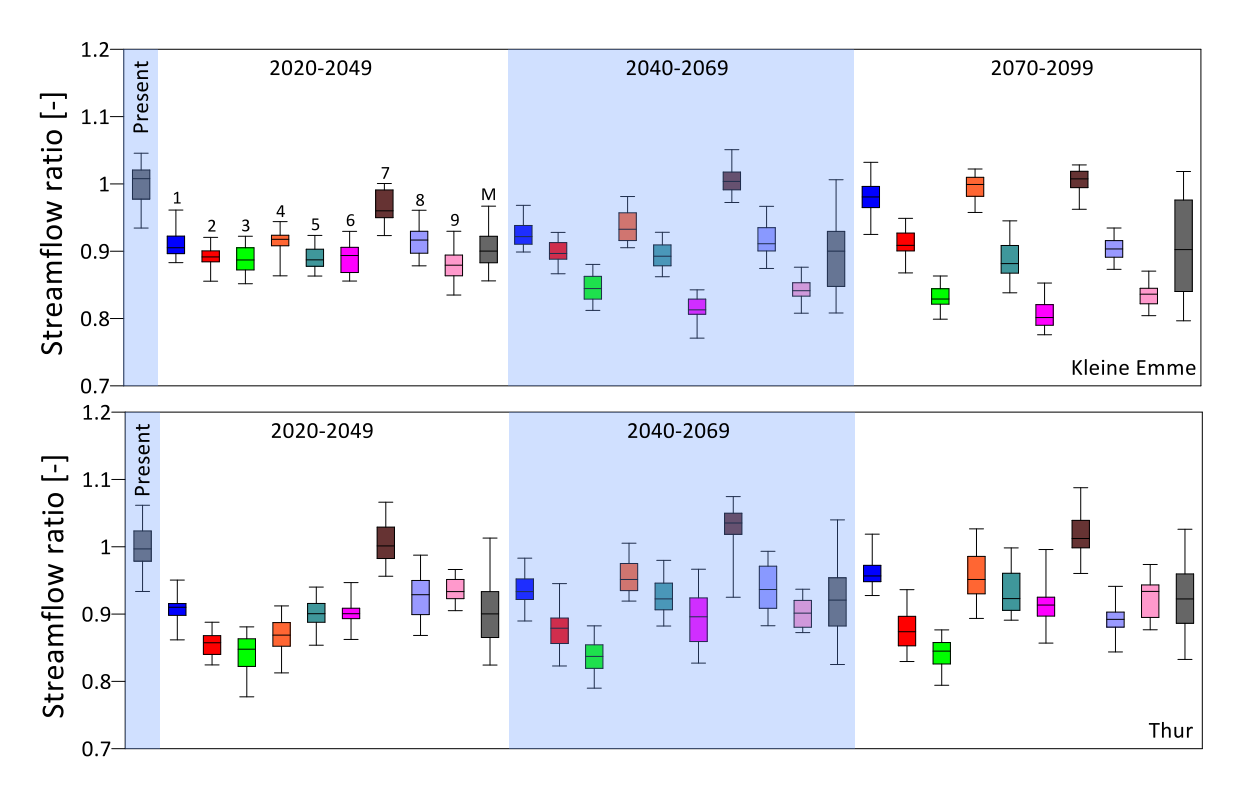


Figure 19 – Differences in mean annual streamflow between the present and future periods for the KI. Emme and Thur catchments. Numbers 1 to 9 refer to the different climate models and M refer to the multi-model mean. Box plots for the present and 1 to 9 represent the stochastic uncertainty for each climate trajectory, and M represents the combination of stochastic and climate model uncertainty. Central lines in the box plots represent the median of mean annual streamflow of the ensemble, while the boxes and whisker lines represent the 25-75th and 5-95th percentile range of the data. The simulated ensemble for each climate trajectory is composed of 30 realizations of 30 years each, bootstrapped from an archive of 100 years.

The changes in the streamflow regime and the larger variability resulting from the simulations suggest possible changes occurring to the internal hydrologic response of the catchments. Examining the changes to the different hydrological component in the catchments (Figure 21), the changes to snow properties (~50 mm deficit per year in future climates) are found to be the most meaningful at the catchment scale. They are one order of magnitude larger than the changes affecting soil wetness and evapotranspiration, which are estimated to be in the order of 5 mm per year, and can explain the projected temporal changes in mean streamflow across the seasons.

A closer analysis of the changes to the snow properties in time and space was conducted by investigating first the changes over the catchments of snow water equivalent (SWE, Figure 22) and then of snow cover (Figure 23). With increasing warming, we expect SWE contribution to the streamflow to reduce with time, and this indeed observed from the results. The decrease in SWE

contribution is already significant for the early-mid-century period for both Kl. Emme (-20%) and Thur (-21%) catchments. At the end of the century, SWE contributes decreases to -57% (Kl. Emme) and -48% (Thur) in comparison to the present values. As foreseen, the high-elevated areas are more prone to the changes in snow coverage and height (Figure 23).

Further analysis of the temporal changes of SWE (Figure 24) reveals that the reduction in SWE at the end-of-the-century for the months of March, April, and May is the main reason for the decrease in mean streamflow at the outlets of Kl. Emme and Thur, thus showing that this decrease is largely dampening the projected increase in precipitation for these months. In the Kl. Emme, it is also evident that the projected increase in precipitation and the reduction of SWE contribution in the winter months (in November, December, and January snowfall is projected to change into rainfall) are both directly responsible for the increase in streamflow.

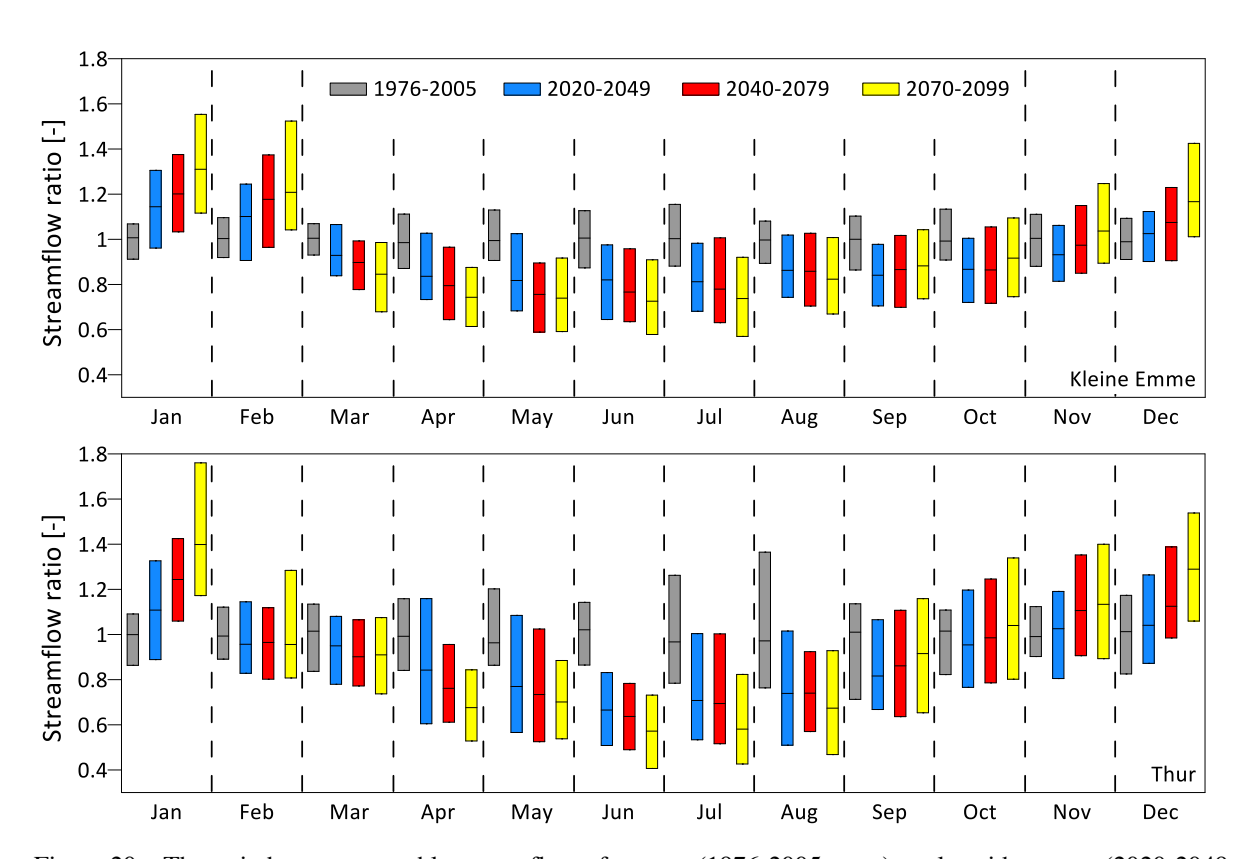


Figure 20 – The ratio between monthly streamflow of present (1976-2005, grey), early-mid-century (2020-2049, blue), mid-century (2040-2079, red) and end of the century (2070-2099, yellow) periods. Box plots for the present period represent the stochastic uncertainty for the future periods represent the combination of stochastic and climate model uncertainty. Central lines in the box plots represent the median of mean monthly streamflow computed from the simulated ensemble, while the boxes represent the 5-95th percentile range of the data. The simulated ensemble for each climate trajectory is composed of 30 realizations of 30 years each, bootstrapped from an archive of 100 years.

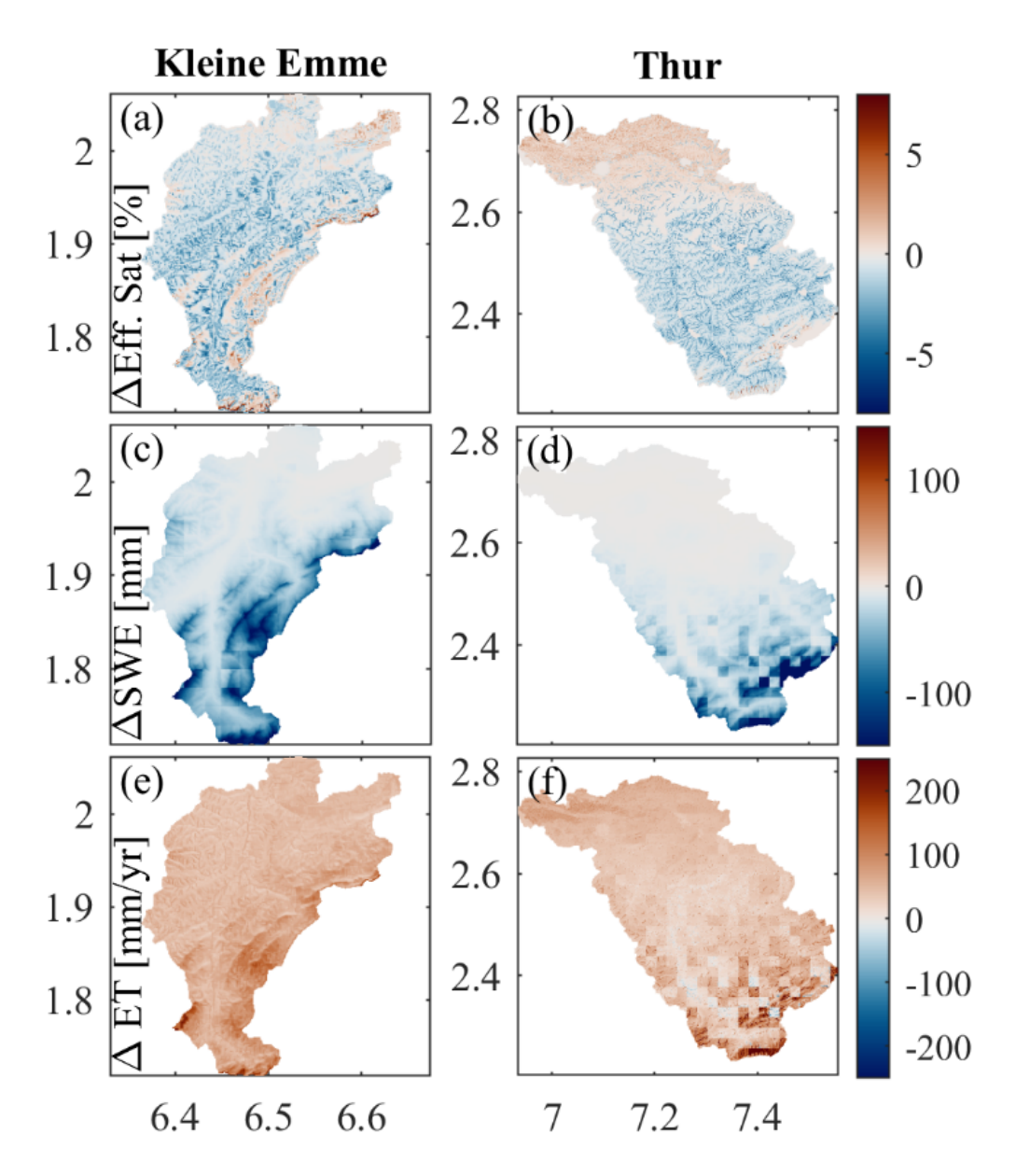


Figure 21 – Change in mean effective saturation (a, b), snow water equivalent (c, d) and annual evapotranspiration (e, f) for the Kl. Emme and Thur catchments. All values correspond to the averages of the multi-model-mean (MMM) at the end of the century (2080–2089) minus the present climate condition.

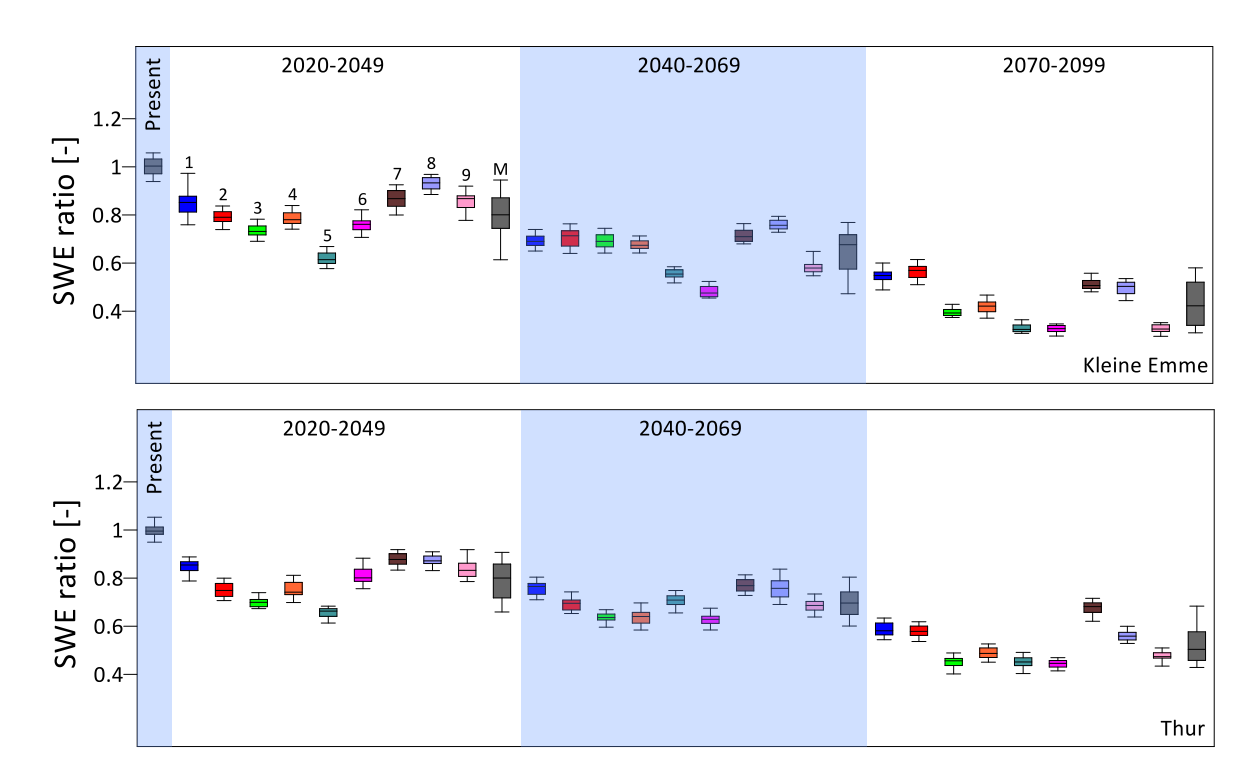


Figure 22 – Differences in snow water equivalent (SWE) between the present and future periods for the K1. Emme and Thur catchments. Numbers 1 to 9 refer to the different climate models and M refer to the multi-model mean. Box plots for the present and 1 to 9 represent the stochastic uncertainty for each climate trajectory, and M represents the combination of stochastic and climate model uncertainty. Central lines in the box plots represent the median of mean SWE of the ensemble, while the boxes and whisker lines represent the 25-75th and 5-95th percentile range of the data. The simulated ensemble for each climate trajectory is composed of 30 realizations of 30 years each, bootstrapped from an archive of 100 years.

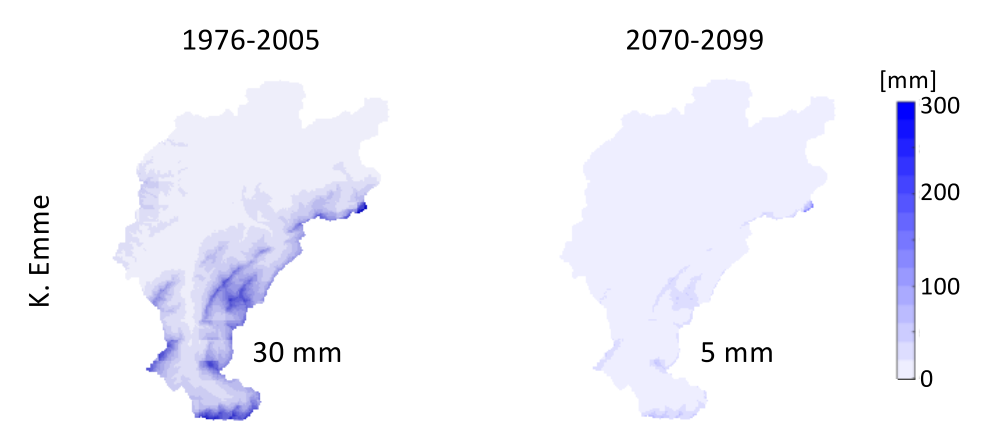


Figure 23 – Average snow height in the Kl. Emme catchment for the present period (left) and end of the century (right, multi-model-mean).

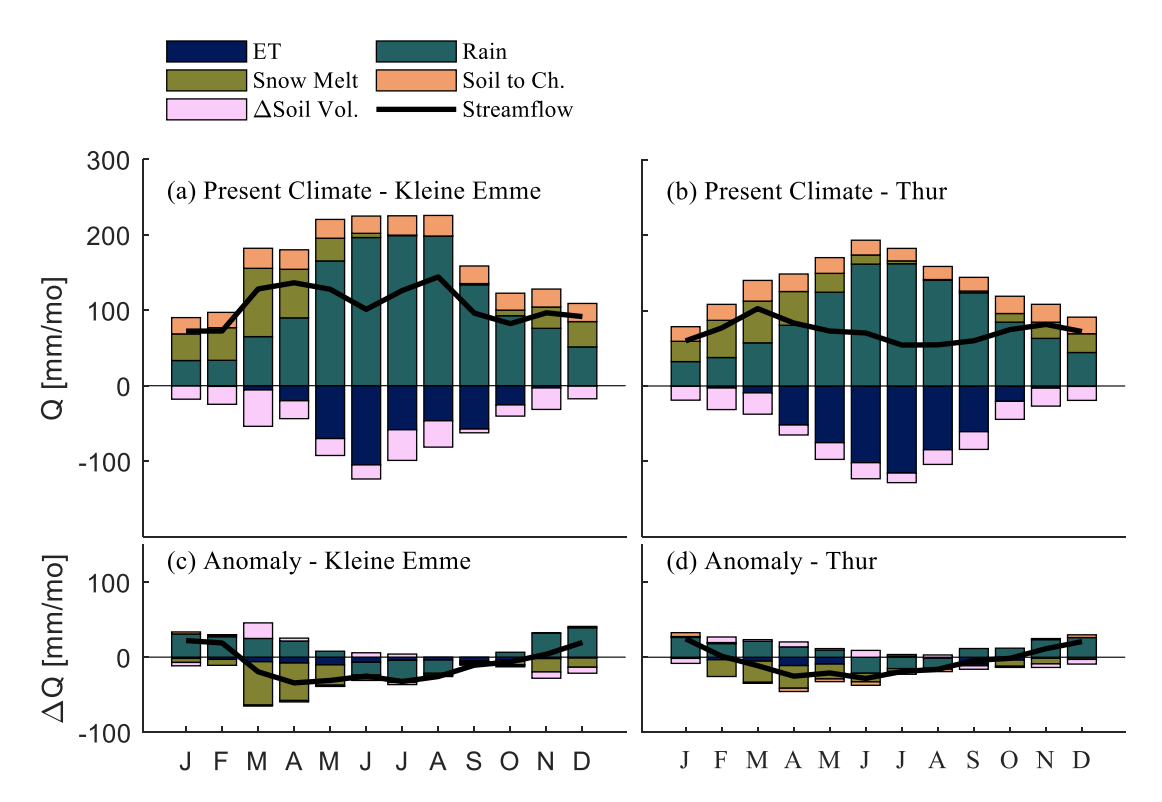


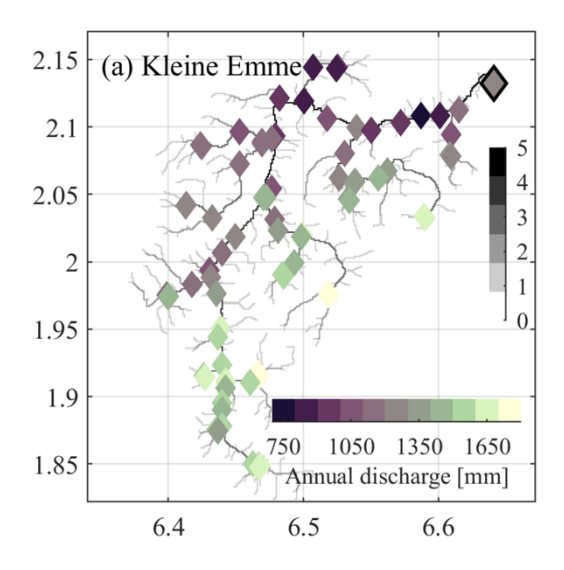
Figure 24 – Monthly streamflow (thick black line) and its hydrological components at the outlet of the Kl. Emme (a, c) and Thur (b, d) river catchments for the present climate (a, b) and the changes projected towards the end of the century (2080–2089, c, d). The bars corresponding to evapotranspiration (blue) and an increase in soil water volume (pink) are depicted as negative contributions to the water balance.

5.4.2 Streamflow heterogeneity within catchments (Kl. Emme and Thur)

The impact on streamflow was investigated also with respect to its variability throughout the river network within the Kl. Emme and Thur catchments. Streamflow was thus analysed for 96 sub-catchment outlets in the Kl. Emme river and 140 ones in the Thur catchment (Figure 25).

Changes to the streamflow were found to be correlated with elevation, especially for the mean and maximum hourly flows (Figure 26). For both the Kl. Emme and the Thur catchments, a significant decrease in the mean streamflow in sub-catchments located at high elevation is projected, while sub-catchments at low elevation show a range of no-change to positive-change in mean streamflow. We note that while in the Kl. Emme the relation between mean streamflow and elevation is almost linear (Figure 26c), in the Thur the relation is following an exponential-like curve (Figure 26d). This can be likely explained by the difference in terrain morphology between the two catchments, as the Kl. Emme is considerably smaller and steeper than the Thur catchment. However, other drivers, such as the properties of soil and vegetation (and land-use) and their spatial distribution can also contribute to the differences in the type of streamflow-elevation relation between the two catchments. The projected changes to the maximum hourly streamflow are exhibiting patterns similar to the mean streamflow, i.e. decrease in high-elevation sub-catchments and increase in low elevation sub-catchments. However, they are characterised by weaker (less correlated) relationship and stronger magnitudes of change (Figure 26a and Figure 26b).

The 7-day low flows are projected to decrease for all sub-catchments in both rivers. While in the Thur the correlation of the magnitude of decrease with elevation is preserved (Figure 26f), in the Kl. Emme catchment the relation seems to break and there is no clear correlation with elevation (Figure 26e).



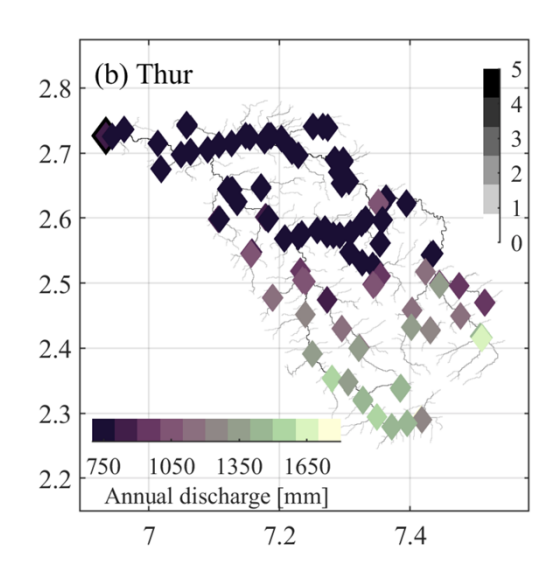


Figure 25 – Spatial distribution of 96 sub-catchments in the Kl. Emme river network (a) and 140 of the Thur river network (b). River reaches are drawn according to their Strahler order and markers are coloured based on their average specific annual discharge in the present climate.

The physically explicit and distributed nature of the hydrological model allows investigating the partitioning of the key hydrological components that drive the streamflow changes and how these are projected to change with elevation (Figure 27). In the Kl. Emme catchment, the main driver for summer streamflow is precipitation and the second is evapotranspiration, both for the present and the end-of-the-century climates. In winter, present-day streamflow is driven by a combination of precipitation, snowmelt and subsurface flow contribution as main drivers, while in the future, precipitation will be the main driver alone. It is also interesting to note that there is an increase in the relative contribution of subsurface lateral flow (denoted as soil-to-channel in Figure 27) to streamflow, especially at the lower elevations, as the second-most-important driver. In autumn, the second-most-important driver changes from subsurface flow contribution to evapotranspiration in the entire elevation range. In spring, the second-most-important driver shifts from snowmelt to evapotranspiration, especially in sub-catchments located at a lower elevation.

These changes, visible also in the Thur catchment (Figure 28), clearly point at the impacts of climate change on various hydrological components in the catchments. In particular, at high elevation, the reduction of snow is the main reason for the changes in streamflow, while evapotranspiration processes dominate at the lower elevations. However, as the changes in snowmelt are four times larger than the changes in evapotranspiration, high-elevation sub-catchments are more sensitive to changes in streamflow (Figure 27 and Figure 28). In summer, the changes to streamflow at all elevations are a direct result of climate change impacts on precipitation, which is the most-

important driver in this season (and overall), and are less affected by the changes to snow, evapotranspiration, and soil water dynamics.

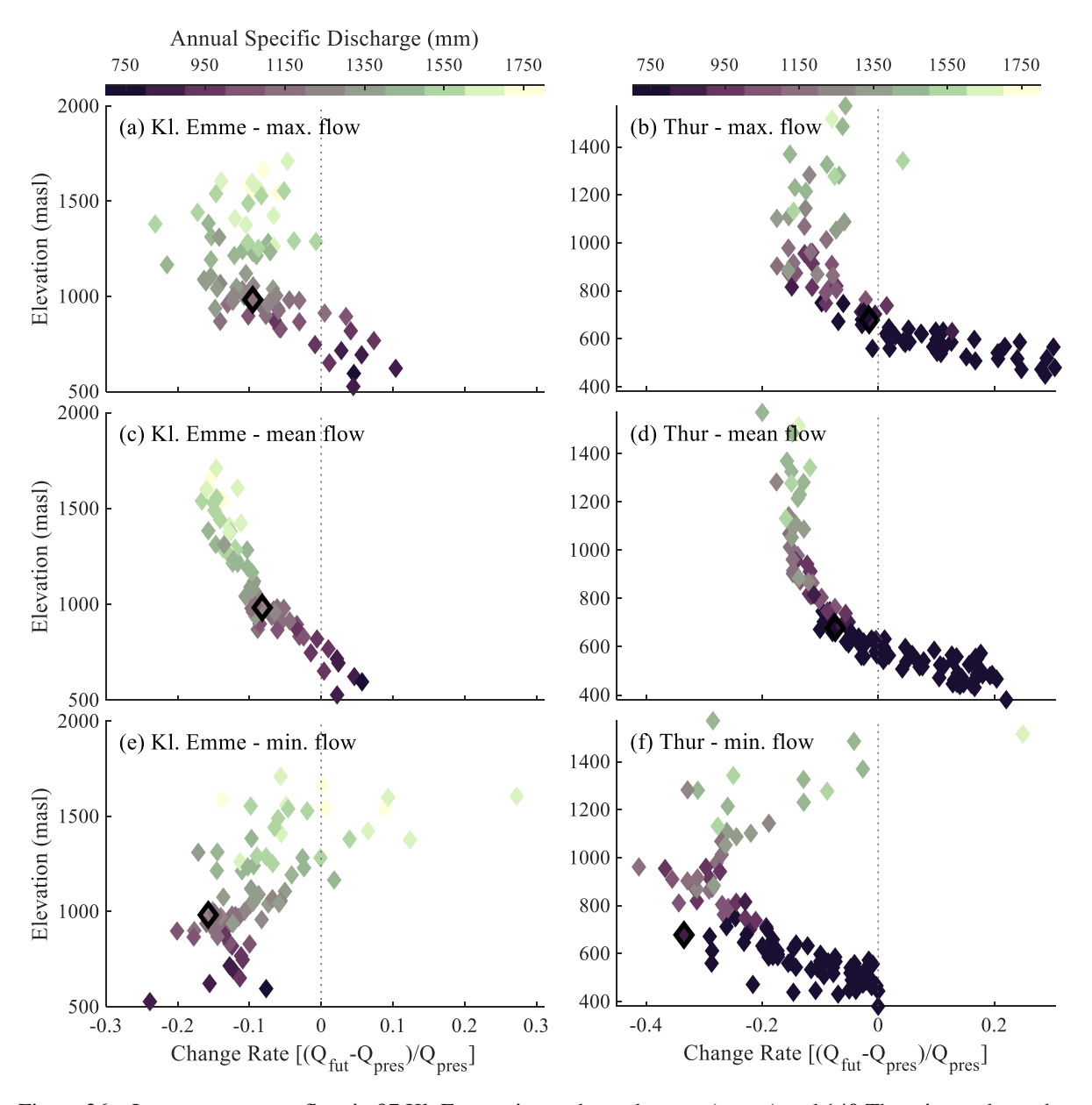


Figure 26 – Impacts on streamflow in 97 Kl. Emme river sub-catchments (a, c, e) and 140 Thur river sub-catchments (b, d, f). The change rates between the present climate and the end of the century are computed for each river section are shown for the maximum hourly flow (a, b), mean flow (c, d) and 7-day minimum flow (e, f). The markers in all plots are colored according to the mean specific streamflow in the present climate, and the river section corresponding to the outlet of the entire catchment is highlighted with a black border.

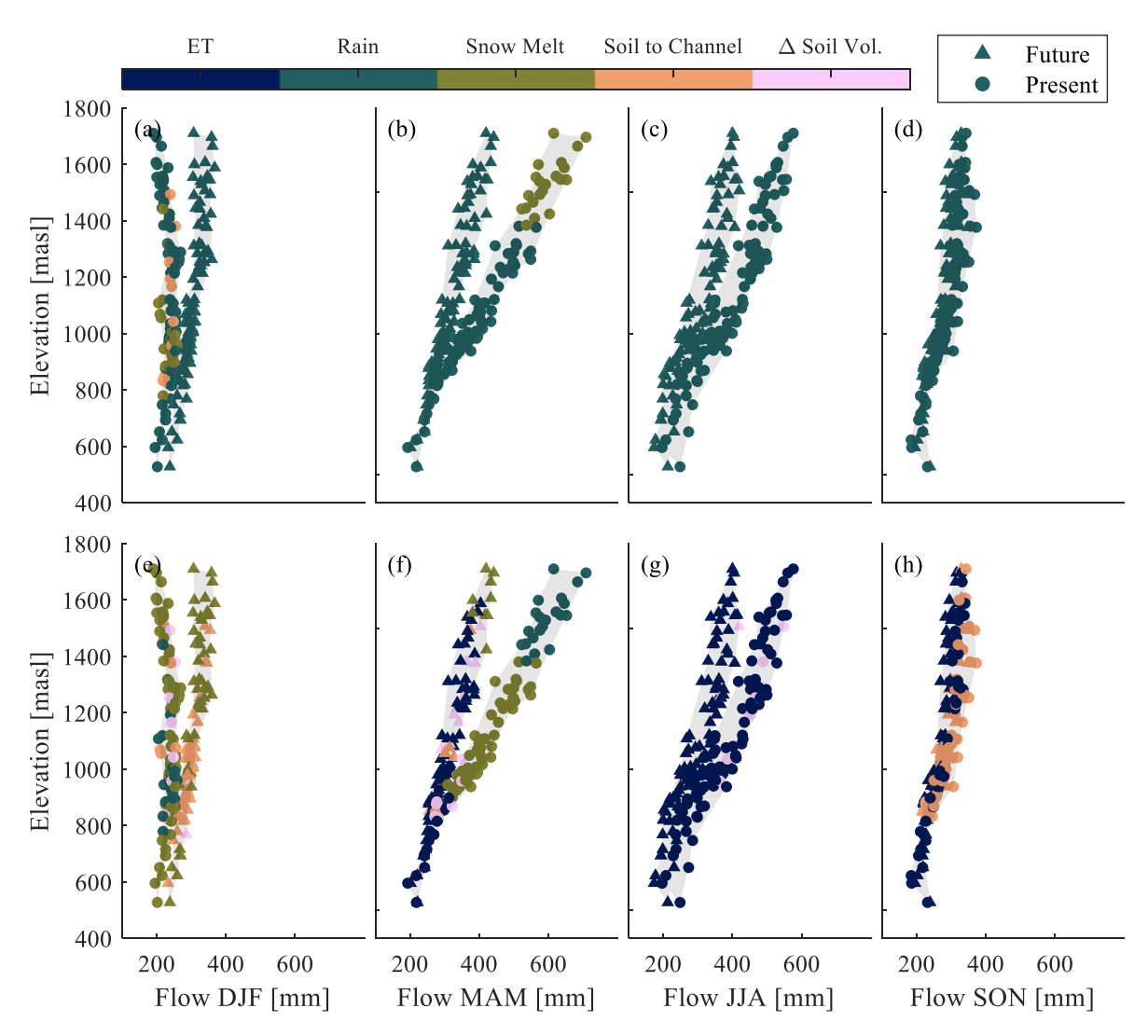


Figure 27 – Most important (a–d) and second most important (e–h) driver of seasonal flow in the Kl. Emme river network under present (circles) and future (triangles) climate conditions.

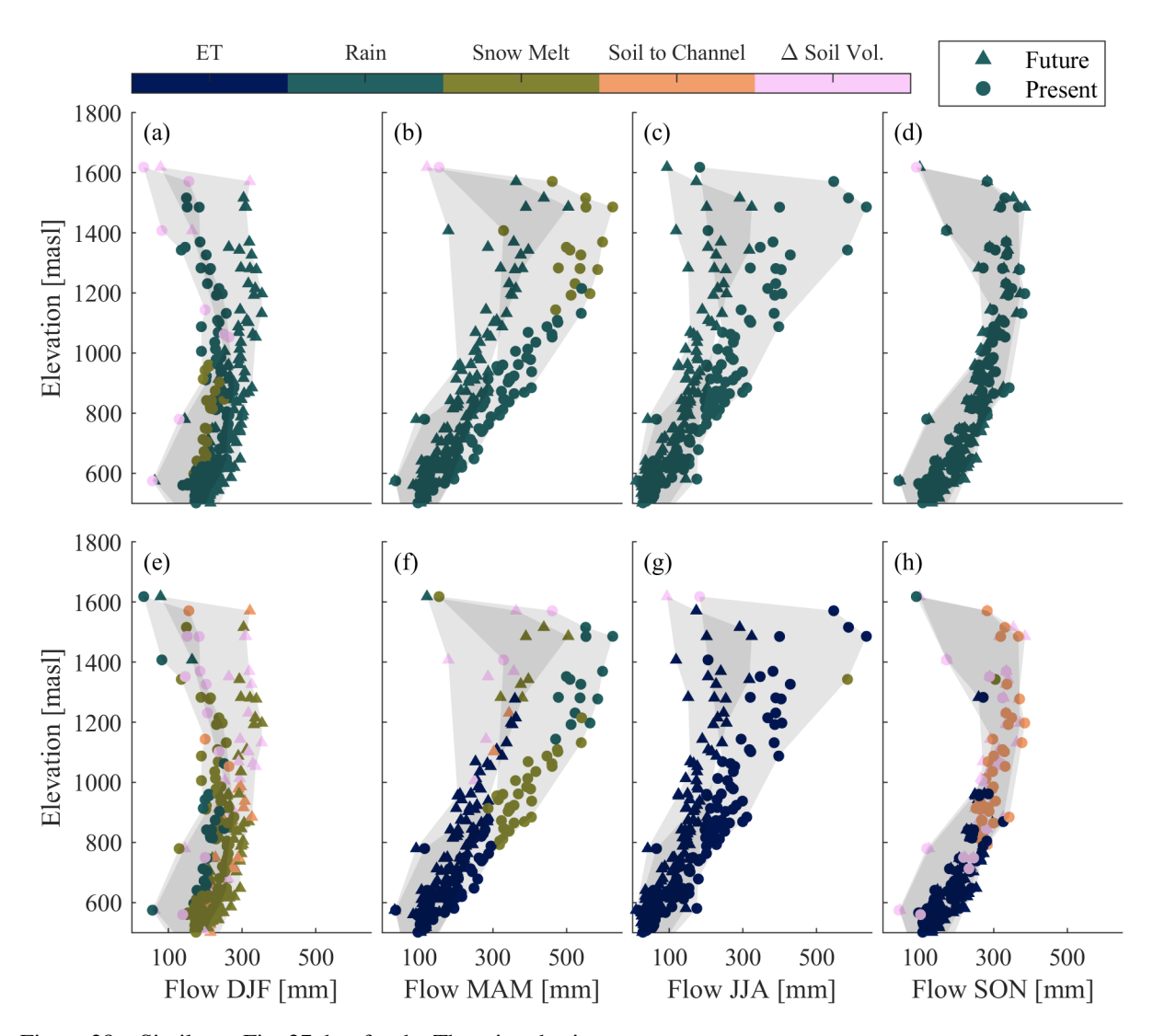


Figure 28 – Similar to Fig. 27, but for the Thur river basin.

5.5 Changes to the Mean Inflows into the Reservoirs in the Maggia Basin

The Maggia river basin is different from the Thur and Kl. Emme not only because of its climatic characteristics, but also because it cannot be considered as a "natural" river. OFIMA¹ operates many reservoirs for hydropower supply, thus inducing a strong regulation of the streamflow regime downstream of the hydropower systems. However, due to the importance of hydropower generation for the electricity supply of Switzerland, the project explored the streamflow response to climate change upstream of the reservoirs, with the purpose of quantifying how changes to the natural system response are expected to impact the inflows at the major reservoir of the hydropower system. Thus, we explored the inflow response to the hydropower reservoirs of Sambuco, Robiei-Zott and Cavagnoli-Naret (see Figure 29). For these reservoirs, we can assume changes in inflow in the future will be a result of changes in climate alone. It must be noted, however, that the complex topology of the intakes leading water these reservoirs and the partial lack of information on flows drained by several of these intakes do not allow accurate calibration of the simulations driven by observed present-day climatology (Figure 9). The comparison between simulations driven by present-day (simulated) and climate change forcing is still meaningful in a relative sense.

Mixed responses to the changes in climate were detected when examining the changes in inflows into the reservoirs in the Maggia river basin (Figure 30 and Figure 31). For Sambuco, most simulations though driven by different models agree on a small reduction of inflows (median reduction of up to 5%), while in Robiei-Zott most simulations agree on an increase in inflows (up to a median of 10%) and in the Cavagnoli-Naret system no significant changes were found. Sambuco has the same seasonal dynamic changes as in the large river systems of K1. Emme and Thur (i.e. a reduction in winter inflows and an increase in summer inflows), while for the two smaller reservoir systems, an increase in inflows up to 20% was found throughout all months.

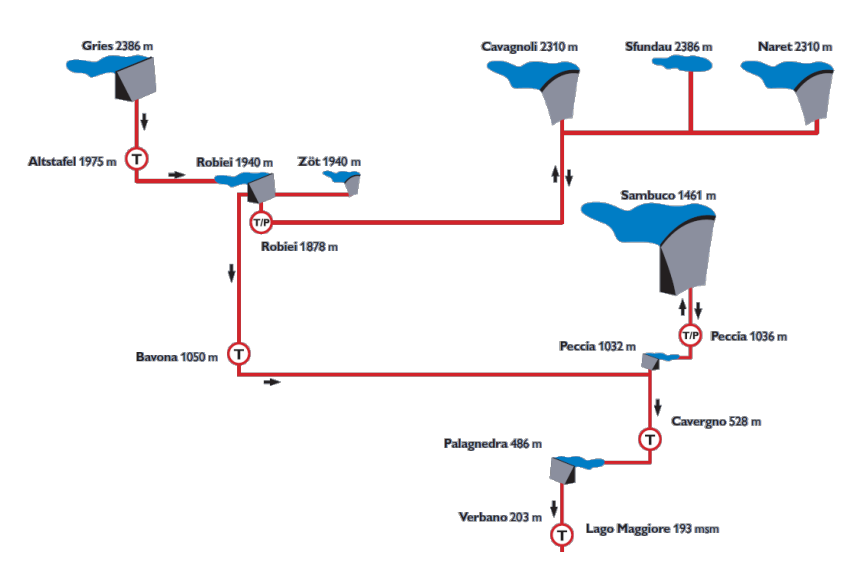


Figure 29 – Schematic representation of the hydro-power reservoirs in the Maggia river basin. Image is from OFIMA website¹.

-

¹ OFficine Idroelettriche della MAggia (www.ofima.ch)

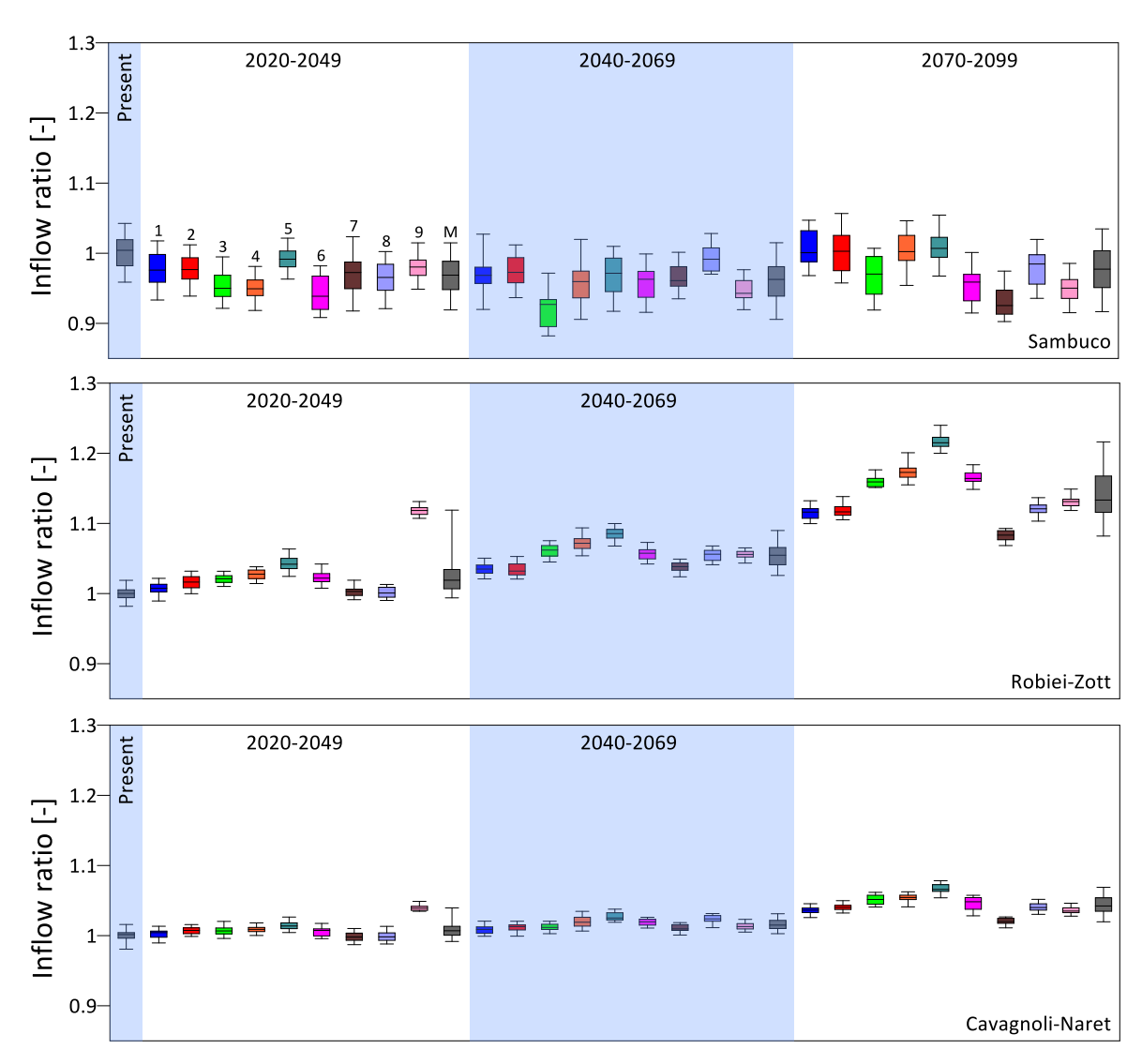


Figure 30 – Differences in mean annual inflow to the reservoirs between the present and future periods. Numbers 1 to 9 refer to the different climate models and M refer to the multi-model mean. Box plots for the present and 1 to 9 represent the stochastic uncertainty for each climate trajectory, and M represents the combination of stochastic and climate model uncertainty. Central lines in the box plots represent the median of mean annual streamflow of the ensemble, while the boxes and whisker lines represent the 25-75th and 5-95th percentile range of the data. The simulated ensemble for each climate trajectory is composed of 30 realizations of 30 years each, bootstrapped from an archive of 100 years.

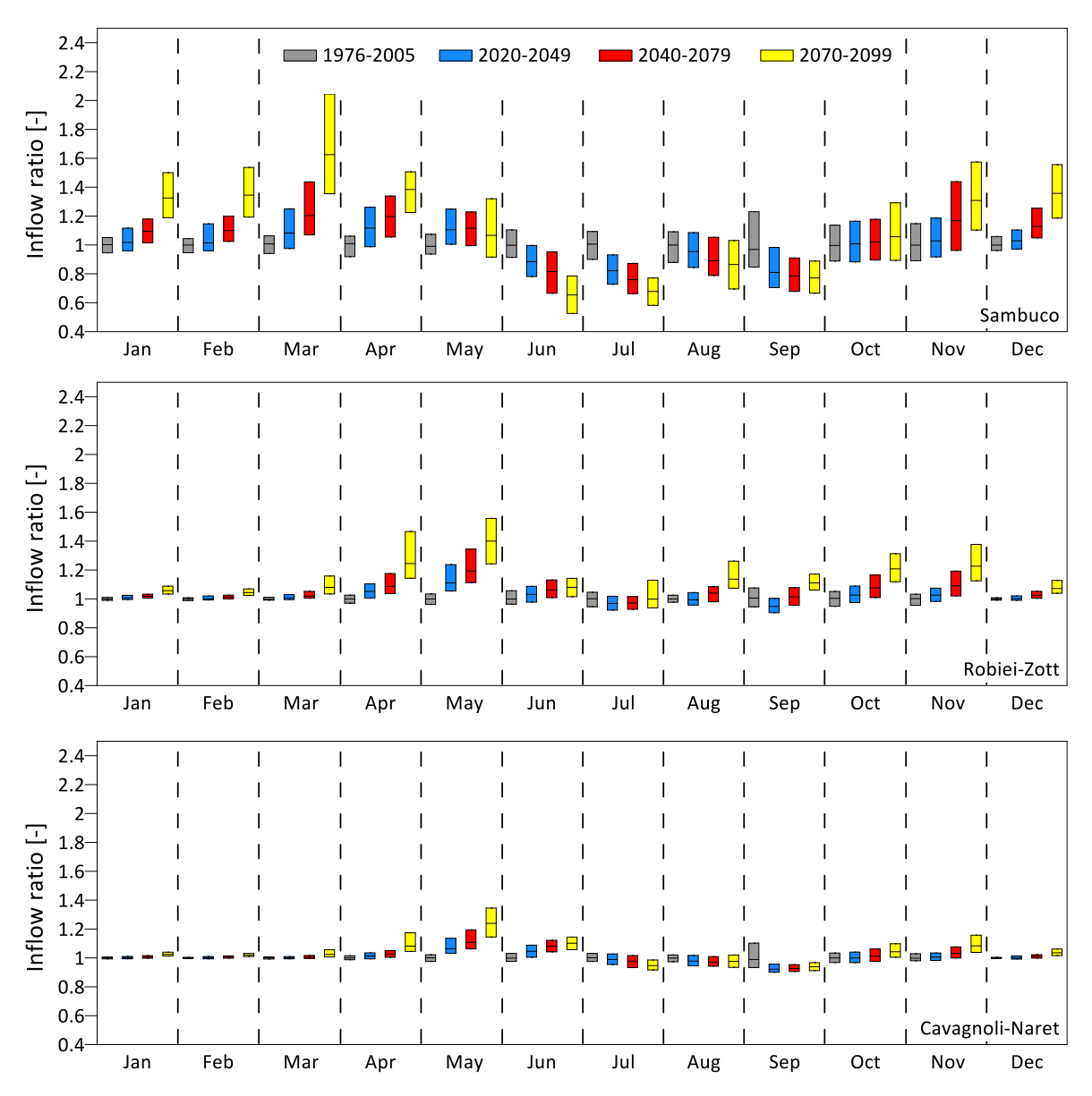


Figure 31 – The ratio between monthly inflow into the reservoirs of the present (1976-2005, grey), early-mid century (2020-2049, blue), mid-century (2040-2079, red) and end of the century (2070-2099, yellow) periods. Box plots for the present period represent the stochastic uncertainty for the future periods represent the combination of stochastic and climate model uncertainty. Central lines in the box plots represent the median of mean monthly streamflow computed from the simulated ensemble, while the boxes represent the 5-95th percentile range of the data. The simulated ensemble for each climate trajectory is composed of 30 realizations of 30 years each, bootstrapped from an archive of 100 years.

5.5.1 Changes to extreme flows in the KI. Emme and Thur

The changes to the extreme flow statistics at the outlet of the Kl. Emme and Thur catchments were explored at the hourly (Figure 32) and daily (Figure 33) scales. Examining the changes to the multi-model mean simulations at the hourly scale, the annual maximum streamflow reduces in the Kl. Emme catchment by -14% (for the 2-year return period) to -12% (30-year return period). In the Thur catchment, the present and future annual maximum streamflow are similar for

all return periods. Similar to the findings of the extreme precipitation analysis, both components of stochastic uncertainty and climate model uncertainty increase with return periods. As a result, the uncertainty range around the multi-model-mean simulations overlaps with the uncertainty of the present climate. Moreover, in many cases, the uncertainty of the simulations driven by downscaled multi-model-mean forcing is even larger than the uncertainty of the present period. Consequently, we can conclude that the statistics of future extreme streamflow fall well within the natural variability characteristic of the present-day climate. Accordingly, we cannot point on a clear negative or positive signal of change in the statistics of future streamflow extreme. The same conclusion is valid for the future annual maximum streamflow on a daily scale.

The temporal changes to the hourly and daily streamflow extremes were also examined (Figure 34), particularly with respect to the seasonal occurrence. Most floods in the Kl. Emme occur historically during summer, regardless of the scale of the analysis, hourly or daily; this holds true also for extreme events at the end of the century (Figure 34a and Figure 34b). However, a shift of many events between summer and other seasons can be detected in the future, when analysing simulations at the hourly scale: the frequency of summer events decreases and is compensated by an increase in the frequency of floods in the other seasons, mainly in winter, though an increase in frequency is also seen in autumn and spring. This is expected as: (i) more precipitation will fall in liquid form rather than solid form; and (ii) there is a potential increase of the rain-on-snow events that are known to trigger floods in high-mountain catchments (Morán-Tejeda et al., 2016). A similar type of change is seen for the Thur at the hourly scale (Figure 34c). At the daily scale (Figure 34d) it seems that flood events in the Thur are more evenly scattered between seasons, even though a reduction in flood events during summer and an increase in flood events in winter is also noticeable.

Finally, we examined the changes for the low flow statistics, using the NM7Q index (Figure 35). As in the case of the statistics of the annual maximum flows, the uncertainty (both stochastic and emerging from the climate models) increases when shifting from the high-frequency events (e.g. 2-year return period) to low-frequency ones (30-year). However, unlike the statistics of the annual maximum streamflow, the simulations driven by the climate trajectories downscaled from the multi-model mean statistics fall outside of the natural variability of present-day for all future periods. This means that most models agree on a reduction in low-flows statistics both in the Kl. Emme and the Thur catchments. The reduction in low-flow statistics is found already in the midearly century period and is reaching its maximum reduction at the end of the century, where the multi-model mean based simulations show a reduction by 25% compared to the mean of present-day in both Kl. Emme and the Thur catchments. As expected, due to the strong seasonality of low flows, there is no change in their seasonal occurrence.

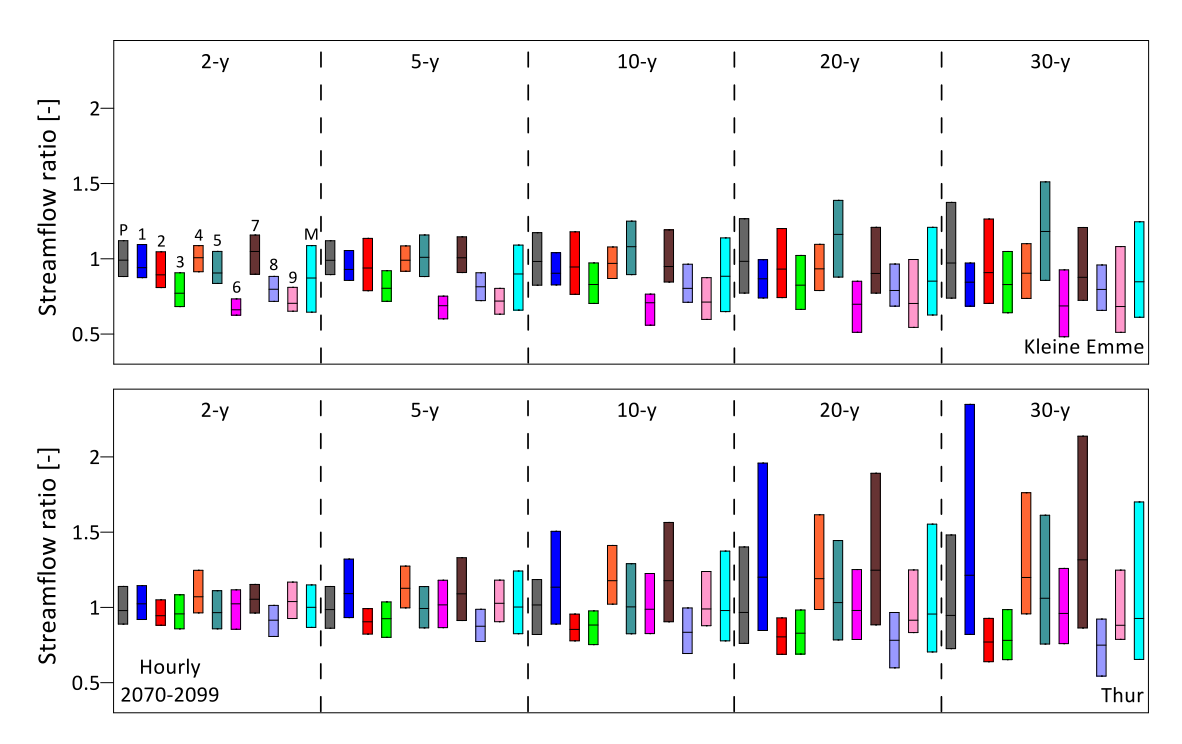


Figure 32 – The ratio between annual maximum streamflow for a given return period of present climate (1976-2005) and end of the century climate (2070-2099) at the hourly scale. Numbers 1 to 9 refer to the different climate models and M refer to the multi-model mean. Box plots for the present and 1 to 9 represent the stochastic uncertainty for each climate trajectory, and M represents the combination of stochastic and climate model uncertainty. Central lines in the box plots represent the median of mean annual maximum streamflow computed from the simulated ensemble using GEV distribution, while the boxes represent the 5-95th percentile range of the data. The simulated ensemble for each climate trajectory is composed of 30 realizations of 30 years each, bootstrapped from an archive of 100 years.

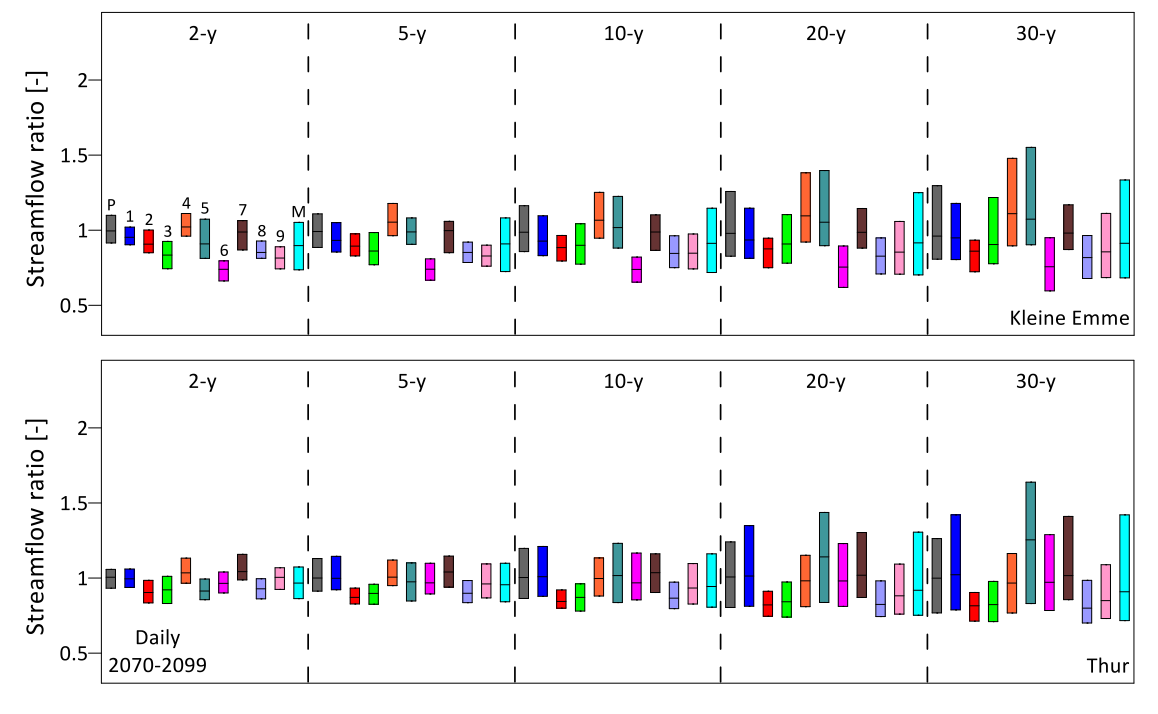


Figure 33 – Similar plot as Fig. 22, but on a daily scale.

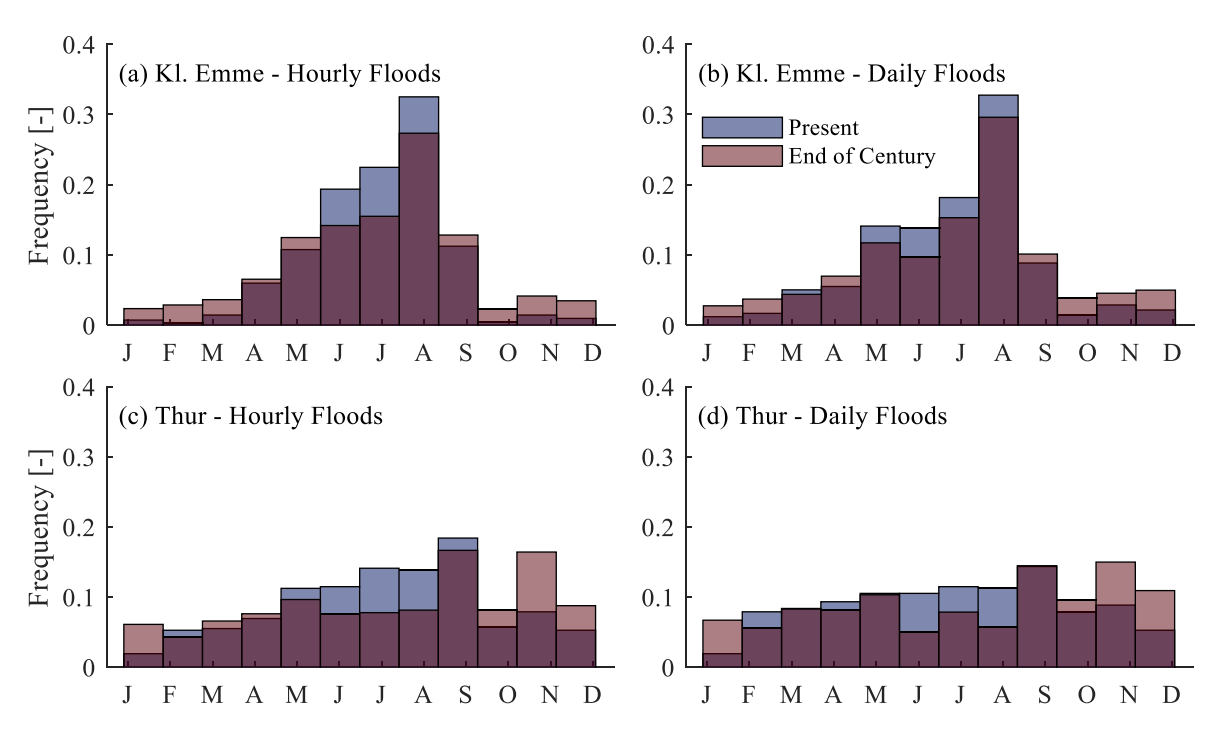


Figure 34 – Monthly frequency of the hourly (a, c) and daily (b, d) maximum yearly outlet streamflow occurring in each month in the Kl. Emme (a-b) and Thur (c-d) rivers.

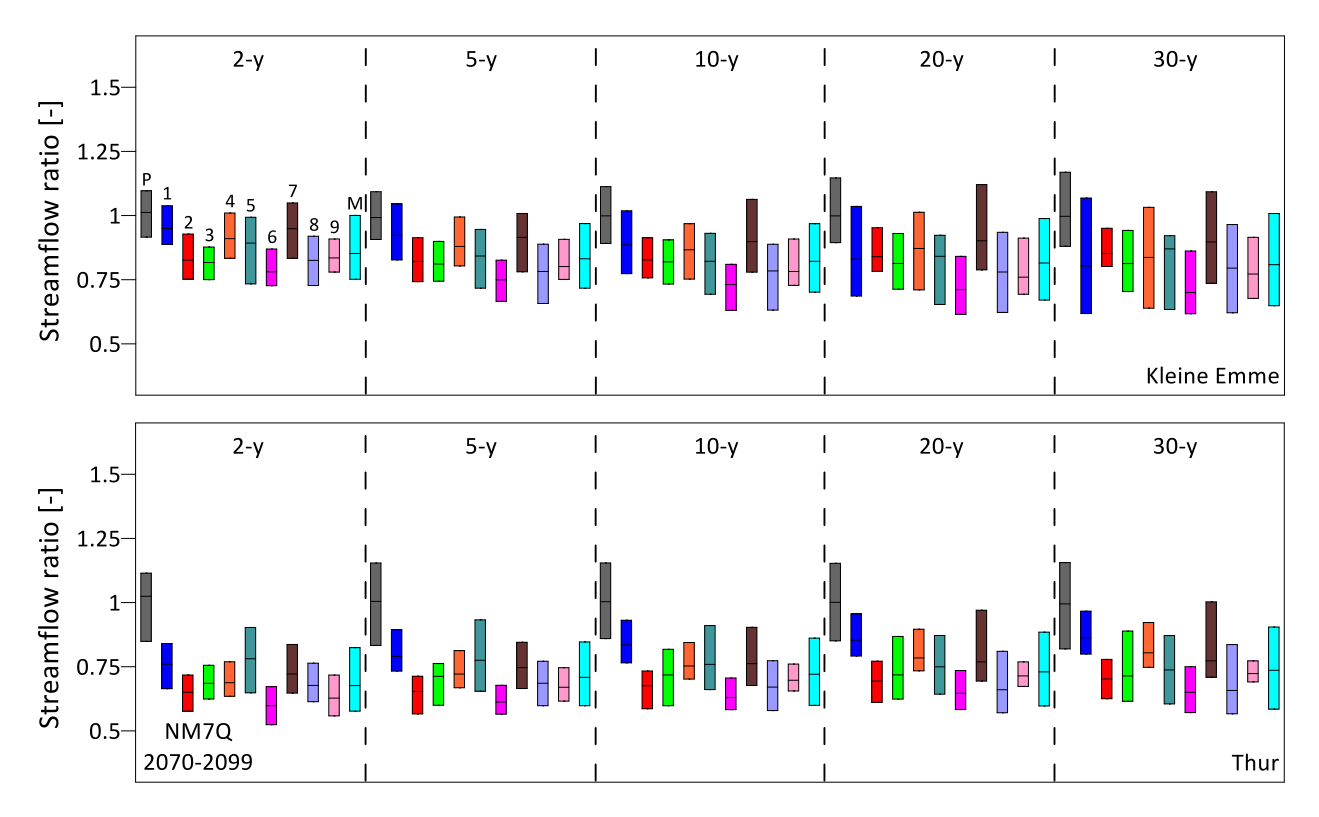


Figure 35 – Similar plot as Fig. 22, but for NM7Q. Note that for the GEV calculation the minimum annual streamflow was multiple by -1.

6 CONCLUSIONS

The key "take-home messages" from this project can be summarised as follows.

Climate

- Temperature is projected to vary almost uniformly in the representative catchments that were explored, while precipitation changes show a non-uniform pattern within the three catchments, with an increase in precipitation projected at lower elevations and decrease projected at higher ones.
- The use of high-resolution climate simulations accounting for the natural variability is key to capture properly the hydrological changes in time and space, and to characterise the entire spectrum of variability and uncertainty.
- Stochastic uncertainty (emerging mainly from the natural variability of precipitation in space and time) and climate model uncertainty components (emerging mainly from the temperature changes) are both meaningful for the characterization of the uncertainties in future streamflow. Stochastic models of climate forcing are therefore needed to adequately estimate the uncertainties associated with the impact of climate change on hydrological compartments.

Streamflow

- A general decrease of outlet streamflow in future periods is seen for the two natural catchments (Kl. Emme and Thur), with the most meaningful change occurring before the mid of the century. Winter streamflow is projected to increase, while summer streamflow simulations exhibit a reduction.
- Changes to streamflow are elevation-dependent: the streamflow in sub-catchments located at high elevation is foreseen to decrease, while the streamflow in sub-catchments located at a lower elevation is projected to remain similar to the present or even slightly increase.
- Changes to snowmelt are the main driver to the changes in streamflow (contribute is four times larger than changes in evapotranspiration or soil-water dynamics). This explains the higher sensitivity of top mountain sub-catchments in comparison to the lower sensitivity of sub-catchments that are close to the outlet.
- The largest of the three reservoirs of the hydropower system in the Maggia (Sambuco) exhibits similar dynamics of the changes as that observed from simulations in the Kl. Emme and Thur, i.e. a general decrease in inflows, seasonally characterised, however, by an increase of winter and a decrease of summer inflows). A different behaviour, namely an increase of both winter and summer inflows characterises the other two and smaller reservoirs, thus underlining the need of spatially highly resolved simulations to capture local changes that would be misinterpreted by generalising the behaviour of a single high-altitude system.

Extremes

- Changes to the extreme streamflow (annual maximum) at the hourly scale are highly uncertain. Most changes fall within the natural (stochastic) variability. Further analyses are required to establish if the magnitudes of hourly extremes are influenced by climate change.
- Floods (at hourly and daily scales) are projected to become less frequent during summer (which will remain the main period of flood occurrences) and more frequent during winter in comparison to the present.

- No changes were found to the structure of the hydrographs during flood events at the hourly scale.
- The magnitude of floods in sub-catchments located in low-elevation is projected to increase, while in sub-catchments located in high-elevation is projected to decrease. The changes to the magnitude of floods in space are following the changes in the magnitude of precipitation in space (i.e. higher precipitation in toward the catchments' outlets), but is also driven by the antecedent soil moisture content, which is projected to increase in low-elevation (i.e. increasing the flood-potential) and decrease in high-elevation.
- Low-flows (7-day streamflow minimum) are projected to reduce by the end of the century.

7 REFERENCES

- Addor, N. et al., 2014. Robust changes and sources of uncertainty in the projected hydrological regimes of Swiss catchments. *Water Resources Research*, 50(10): 7541-7562.
- Battista, G., Molnar, P., Burlando, P., 2020. Modelling impacts of spatially variable erosion drivers on suspended sediment dynamics. *Earth Surface Dynamics*, 8(3): 619-635.
- CH2011, 2011. Swiss climate change scenarios CH2011, ETH Zurich.
- CH2018, 2018. CH2018-Climate Scenarios for Switzerland-Technical Report.
- CH-Impacts, 2014. Toward quantitative scenarios of climate change Impacts in Switzerland. OCCR, FOEN, MeteoSwiss, Center for Climate Systems Modeling, Agroscope.
- Ciarapica, L., Todini, E., 2002. TOPKAPI: A model for the representation of the rainfall-runoff process at different scales. *Hydrological Processes*, 16(2): 207-229.
- Deser, C., Phillips, A., Bourdette, V., Teng, H., 2012. Uncertainty in climate change projections: the role of internal variability. *Climate dynamics*, 38(3-4): 527-546.
- Fatichi, S., Ivanov, V.Y., Caporali, E., 2011. Simulation of future climate scenarios with a weather generator. *Advances in Water Resources*, 34(4): 448-467.
- Fatichi, S. et al., 2016a. Uncertainty partition challenges the predictability of vital details of climate change. *Earth's Future*, 4(5): 240-251.
- Fatichi, S., Rimkus, S., Burlando, P., Bordoy, R., 2014. Does internal climate variability overwhelm climate change signals in streamflow? The upper Po and Rhone basin case studies. *Science of the Total Environment*, 493: 1171-1182.
- Fatichi, S., Rimkus, S., Burlando, P., Bordoy, R., Molnar, P., 2015. High-resolution distributed analysis of climate and anthropogenic changes on the hydrology of an Alpine catchment. *Journal of Hydrology*, 525: 362-382.
- Fatichi, S. et al., 2016b. An overview of current applications, challenges, and future trends in distributed process-based models in hydrology. *Journal of Hydrology*, 537: 45-60.
- Frei, C., 2014. Interpolation of temperature in a mountainous region using nonlinear profiles and non-Euclidean distances. *International Journal of Climatology*, 34(5): 1585-1605.
- Gabella, M., Bolliger, M., Germann, U., Perona, G., 2005. Large sample evaluation of cumulative rainfall amounts in the Alps using a network of three radars. *Atmospheric research*, 77(1-4): 256-268.

- Gelaro, R. et al., 2017. The modern-era retrospective analysis for research and applications, version 2 (MERRA-2). *Journal of Climate*, 30(14): 5419-5454.
- Germann, U., Galli, G., Boscacci, M., Bolliger, M., 2006. Radar precipitation measurement in a mountainous region. *Quarterly Journal of the Royal Meteorological Society*: A journal of the atmospheric sciences, applied meteorology and physical oceanography, 132(618): 1669-1692.
- Hilker, N., Badoux, A., Hegg, C., 2009. The Swiss flood and landslide damage database 1972–2007. *Nat. Hazards Earth Syst. Sci.*, 9(3): 913-925. DOI:10.5194/nhess-9-913-2009
- Hingray, B., Saïd, M., 2014. Partitioning Internal Variability and Model Uncertainty Components in a Multimember Multimodel Ensemble of Climate Projections. *Journal of Climate*, 27(17): 6779-6798. DOI:10.1175/jcli-d-13-00629.1
- Holben, B.N. et al., 1998. AERONET—A federated instrument network and data archive for aerosol characterization. *Remote sensing of environment*, 66(1): 1-16.
- Jacob, D. et al., 2014. EURO-CORDEX: new high-resolution climate change projections for European impact research. *Regional environmental change*, 14(2): 563-578.
- Keller, D.E. et al., 2015. Implementation and validation of a Wilks-type multi-site daily precipitation generator over a typical Alpine river catchment. *Hydrology and Earth System Sciences*, 19(5): 2163-2177.
- Morán-Tejeda, E., López-Moreno, J.I., Stoffel, M., Beniston, M., 2016. Rain-on-snow events in Switzerland: recent observations and projections for the 21st century. *Climate Research*, 71(2): 111-125.
- Pappas, C., Fatichi, S., Rimkus, S., Burlando, P., Huber, M.O., 2015. The role of local-scale heterogeneities in terrestrial ecosystem modeling. *Journal of Geophysical Research*: Biogeosciences, 120(2): 341-360.
- Paschalis, A., Fatichi, S., Molnar, P., Rimkus, S., Burlando, P., 2014. On the effects of small scale space—time variability of rainfall on basin flood response. *Journal of Hydrology*, 514: 313-327.
- Peleg, N., Fatichi, S., Paschalis, A., Molnar, P., Burlando, P., 2017. An advanced stochastic weather generator for simulating 2-D high-resolution climate variables. *Journal of Advances in Modeling Earth Systems*, 9(3): 1595-1627.
- Peleg, N., Molnar, P., Burlando, P., Fatichi, S., 2019. Exploring stochastic climate uncertainty in space and time using a gridded hourly weather generator. *Journal of Hydrology*, 571: 627-641.
- Peleg, N., Sinclair, S., Fatichi, S., Burlando, P., 2020. Downscaling climate projections over large and data sparse regions: Methodological application in the Zambezi River Basin. *International Journal of Climatology*.
- Ragettli, S., Cortés, G., McPhee, J., Pellicciotti, F., 2014. An evaluation of approaches for modelling hydrological processes in high-elevation, glacierized Andean watersheds. *Hydrological Processes*, 28(23): 5674-5695.
- Rajczak, J., Kotlarski, S., Schär, C., 2016. Does quantile mapping of simulated precipitation correct for biases in transition probabilities and spell lengths? *Journal of Climate*, 29(5): 1605-1615.
- Scherrer, S.C. et al., 2016. Emerging trends in heavy precipitation and hot temperature extremes in Switzerland. *Journal of Geophysical Research*: Atmospheres, 121(6): 2626-2637.
- Schwarb, M., 2000. The Alpine precipitation climate: evaluation of a high-resolution analysis scheme using comprehensive rain-gauge data, ETH Zurich.

Skinner, C.J. et al., 2020. The impact of different rainfall products on landscape modelling simulations. *Earth Surface Processes and Landforms*, 45(11): 2512-2523.

Todini, E., Ciarapica, L., 2001. The TOPKAPI model. In: *Mathematical models of large watershed hydrology*: 471-506, V.P. Singh et al. (Eds.). Water Resources Publications, Littleton, Colorado.